Am J Physiol Heart Circ Physiol 296: H1804–H1810, 2009.
First published April 3, 2009; doi:10.1152/ajpheart.01033.2008.

Endogenous cardiac natriuretic peptides protect the heart in a mouse model of dilated cardiomyopathy and sudden death

Shinji Yasuno,[1] Satoru Usami,[1] Koichiro Kuwahara,[1] Michio Nakanishi,[1] Yuji Arai,[2] Hideyuki Kinoshita,[1] Yasuaki Nakagawa,[1] Masataka Fujiwara,[1] Masao Murakami,[1] Kenji Ueshima,[3] Masaki Harada,[1] and Kazuwa Nakao[1]

[1]*Department of Medicine and Clinical Science, Kyoto University Graduate School of Medicine, Kyoto;* [2]*Department of Biophysics, National Cardiovascular Center Research Institute, Suita; and* [3]*EBM Research Center, Kyoto University Graduate School of Medicine, Kyoto, Japan*

Submitted 26 September 2008; accepted in final form 1 April 2009

Yasuno S, Usami S, Kuwahara K, Nakanishi M, Arai Y, Kinoshita H, Nakagawa Y, Fujiwara M, Murakami M, Ueshima K, Harada M, Nakao K. Endogenous cardiac natriuretic peptides protect the heart in a mouse model of dilated cardiomyopathy and sudden death. *Am J Physiol Heart Circ Physiol* 296: H1804–H1810, 2009. First published April 3, 2009; doi:10.1152/ajpheart.01033.2008.—Ventricular myocytes are known to show increased expression of the cardiac hormones atrial and brain natriuretic peptide (ANP and BNP, respectively) in response to pathological stress on the heart, but their function during the progression of nonischemic dilated cardiomyopathy remains unclear. In this study, we crossed a mouse model of dilated cardiomyopathy and sudden death, which we generated by cardioselectively overexpressing a dominant-negative form of the transcriptional repressor neuron-restrictive silencer factor (dnNRSF Tg mice), with mice lacking guanylyl cyclase-A (GC-A), a common receptor for ANP and BNP, to assess the effects of endogenously expressed natriuretic peptides during progression of the cardiomyopathy seen in dnNRSF Tg mice. We found that dnNRSF Tg;GC-A$^{-/-}$ mice were born normally, but then most died within 4 wk. The survival rates among dnNRSF Tg;GC-A$^{+/-}$ and dnNRSF Tg mice were comparable, but dnNRSF Tg;GC-A$^{+/-}$ mice showed greater systolic dysfunction and a more severe cardiomyopathic phenotype than dnNRSF Tg mice. Collectively, our findings suggest that endogenous ANP/BNP protects the heart against the death and progression of pathological remodeling in a mouse model of dilated cardiomyopathy and sudden death.

neuron-restrictive silencer factor; guanylyl cyclase-A; cardiomyopathy; sudden death

HEART FAILURE IS A LEADING cause of mortality and morbidity in the Western world (17). In United States, for example, ~550,000 new cases are diagnosed each year (12). Despite recent progress in both medical and surgical management, heart failure remains an extremely lethal condition associated with a very poor quality of life and a 5-year survival rate of only ~50% (12, 34). Therefore, a better understanding of the molecular mechanisms underlying the progression of heart failure would be highly desirable, since it could serve as the basis for developing novel therapeutic approaches to treating the ailment.

Heart failure is accompanied by dysregulation of myocardial expression of a set of cardiac genes. One of the best-characterized genetic alterations seen in failing ventricles is reactivation of fetal cardiac genes, including those encoding atrial natriuretic peptide (ANP), skeletal α-actin, and β-myosin heavy chain, which are active within the fetal ventricles but quiescent in normal postnatal ventricles (3, 26). Such transcriptional alterations have been shown to correlate with deterioration of cardiac function and, conversely, improvement of cardiac function in response to medical and/or nonmedical interventions is accompanied by normalization of these genetic alterations (1, 2, 15, 17). Thus reprogramming cardiac gene expression appears to modify the pathological process during the progression of heart failure.

ANP is a cardiac hormone usually synthesized in the atrium and released in response to wall stretch. Upon its release, ANP acts at multiple sites to exert diuretic, natriuretic, and vasorelaxant effects (21). These biological properties are shared by brain natriuretic peptide (BNP), which, despite its name, is primarily secreted from the ventricles (18, 23, 31). Moreover, recent evidence indicates that ANP and BNP also act as paracrine factors, exerting antihypertrophic and antifibrotic effects in the heart (5, 9, 14, 24, 29). They exert both their hormonal and paracrine effects through activation of their common receptor, guanylyl cyclase-A receptor (GC-A), also known as natriuretic peptide receptor-A, which is expressed in a variety of tissues, including kidneys, blood vessels, adrenal glands, and heart (22), and is coupled to an increase in the intracellular concentration of cGMP (10). Ventricular expression of both ANP and BNP is upregulated in several pathological conditions of the heart, and their plasma concentrations are markedly elevated in patients with congestive heart failure (CHF). In fact, measurements of plasma ANP and BNP levels are used clinically to assist in the diagnosis of CHF, to assess prognosis, and to determine therapeutic strategy (16, 27, 30, 33). In addition, ANP and BNP are already being used to treat patients with acute heart failure (4, 32).

We recently found that, following myocardial infarction, mice lacking GC-A showed a higher incidence of acute heart failure, more severe left ventricular (LV) remodeling, and greater impairment of LV systolic function than mice expressing GC-A (20). This suggests that endogenous ANP/BNP may protect heart after myocardial infarction, but the role of intrinsic ANP/BNP signaling during the development of nonischemic dilated cardiomyopathy remains unclear. To address that question, in this study, we crossed a transgenic (Tg) mouse cardioselectively overexpressing a dominant-negative form of the transcriptional repressor neuron-restrictive silencer factor (dnNRSF Tg mice), which is a mouse model of dilated cardiomyopathy and sudden death, with mice lacking GC-A (GC-A$^{-/-}$; see Ref. 11). Almost all of dnNRSF Tg;GC-A$^{-/-}$

Address for reprint requests and other correspondence: K. Kuwahara, Kyoto Univ. Graduate School of Medicine, Dept. of Medicine and Clinical Science, 54 Shogoin Kawaharacho, Sakyo-ku, Kyoto, Japan 606-8507 (e-mail: kuwa@kuhp.kyoto-u.ac.jp).

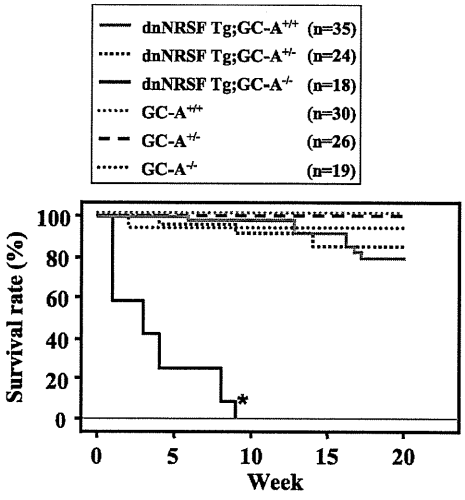

Fig. 1. Kaplan-Meier analysis of survival after birth among guanylyl cyclase-A (GC-A)-sufficient (GC-A$^{+/+}$) mice, GC-A heterozygous knockout (GC-A$^{+/-}$) mice, mice lacking GC-A (GC-A$^{-/-}$), mice overexpressing a dominant-negative form of the transcriptional repressor neuron-restrictive silencer factor (dnNRSF Tg);GC-A$^{+/+}$, dnNRSF Tg;GC-A$^{+/-}$, and dnNRSF Tg;GC-A$^{-/-}$ mice. dnNRSF Tg line 474 was used in this study. *$P < 0.05$ vs. dnNRSF Tg;GC-A$^{+/-}$. *n*, No. of mice.

mice died by 4 wk after birth. The survival rates among dnNRSF Tg;GC-A$^{+/-}$ and dnNRSF Tg mice were comparable, but dnNRSF Tg;GC-A$^{+/-}$ mice showed greater systolic dysfunction and a more severe cardiomyopathic phenotype than dnNRSF Tg mice. These findings suggest that endogenous ANP/BNP protects the heart against the sudden death and the progression of pathological remodeling in the mouse model of dilated cardiomyopathy.

MATERIAL AND METHODS

Animals. The animal care and all experimental protocols were reviewed and approved by the Animal Research Committee in the Kyoto University Graduate School of Medicine. GC-A knockout (KO) mice generated as described previously were kindly provided by D. L. Garbers (The University of Texas Southwestern Medical Center) (14). Using methods described previously (11), we established two dnNRSF Tg lines (471 and 474) having different survival rates. In the present study, we used dnNRSF Tg line 474, whose survival rate was ~80% at 20 wk of age. The GC-A KO (GC-A$^{-/-}$), GC-A heterozygous KO (GC-A$^{+/-}$), dnNRSF Tg;GC-A$^{-/-}$, and dnNRSF Tg;GC-A$^{+/-}$ mice used to examine effects on survival were generated by crossing male GC-A$^{-/-}$ mice and female dnNRSF Tg;GC-A$^{+/-}$ mice. The wild-type (WT), GC-A$^{+/-}$, dnNRSF Tg, and dnNRSF Tg;GC-A$^{+/-}$ mice used in other experiments were generated by crossing male GC-A$^{+/-}$ mice and female dnNRSF Tg;GC-A$^{+/-}$ mice. The genetic background of the original GC-A KO and dnNRSF Tg mice was C57BL/6.

Echocardiographic and hemodynamic analyses. After anesthetizing mice by intraperitoneal injection of a 2.5% wt/vol solution (8 μl/g) of tribromoethanol/amylene hydrate (Avertin), echocardiography was carried out using a Toshiba Power Vision 8000 echocardiographic system equipped with a 12-MHz imaging transducer as described previously (11). For hemodynamic analyses, mice were intubated and anesthetized with 0.5–1.5% isoflurane. A 2-French Millar Micro-Tip catheter (Millar Instruments) was then inserted in the right carotid artery and advanced in the left ventricle to record LV systolic and diastolic pressures, as well as the maximum and minimum rates of LV pressure development (dP/d*t*) (7).

Histological examination. Hearts were fixed in 10% formalin and prepared for histological analysis as described previously (13).

Quantitative RT-PCR analysis. Using 1- or 50-ng samples of total RNA prepared from ventricles, levels of mRNA encoding mouse ANP and BNP; skeletal α-actin; sarco(endo)plasmic reticulum Ca^{2+}-ATPase (SERCA) 2; hyperpolarization-activated cyclic nucleotide-gated potassium channel (HCN) 2 and HCN4, which encode channels that carry the hyperpolarization-activated current; calcium channel, voltage-dependent, T-type, α1H-subunit (CACNA1H), which encodes the α_1H T-type Ca^{2+} channel; GC-A; and glyceraldehyde-3-phosphate dehydrogenase (GAPDH) were then determined by quantitative real-time PCR following the manufacturer's protocol (Applied Biosystems, Zaventam, Belgium) as described previously (20). The real-time PCR primers and probes for ANP, BNP, skeletal α-actin, SERCA2, HCN2, HCN4, CACNA1H, GC-A, and GAPDH were all purchased from Applied Biosystems.

Statistical analysis. Data are presented as means ± SE. ANOVA was used to make multiple group comparisons. If ANOVA showed a significant difference ($P < 0.05$), a post hoc Fisher least-significant difference test was used to identify which group differences accounted for the significant *P* value. Survival rate was analyzed using the

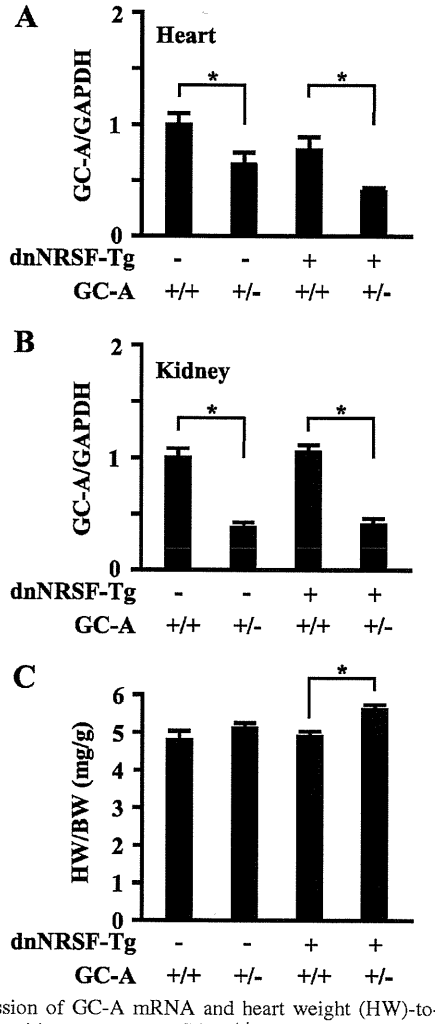

Fig. 2. Expression of GC-A mRNA and heart weight (HW)-to-body weight (BW) ratios (mg/g) in wild-type, GC-A$^{+/-}$, dnNRSF Tg, and dnNRSF-Tg;GC-A$^{+/-}$ mice. *A* and *B*: expression of GC-A mRNA of the heart (*A*) and the kidney (*B*) in wild-type, GC-A$^{+/-}$, dnNRSF Tg, and dnNRSF-Tg;GC-A$^{+/-}$ mice. GAPDH, glyceraldehyde-3-phosphate dehydrogenase. *$P < 0.05$. *C*: HW-to-BW ratios (mg/g) in wild-type, GC-A$^{+/-}$, dnNRSF Tg, and dnNRSF-Tg;GC-A$^{+/-}$ mice. Note that the ratio is significantly increased in dnNRSF Tg;GC-A$^{+/-}$ mice. *$P < 0.05$.

Kaplan-Meier method with the log-rank test. Values of $P < 0.05$ were considered significant.

RESULTS

Loss of GC-A is perinatally lethal in dnNRSF Tg mice. To determine the effects of the increased cardiac expression of ANP/BNP during the development and progression of dilated cardiomyopathy leading to sudden death, we generated dnNRSF Tg mice having a GC-A-null background by crossing dnNRSF Tg (line 474) with GC-A$^{-/-}$ mice (14). The resultant dnNRSF Tg;GC-A$^{-/-}$ mice were born at a rate similar to GC-A$^{-/-}$ mice. Moreover, the heart weight-to-body weight ratios on *postnatal day 2* did not differ significantly between the two genotypes (data not shown). Both dnNRSF Tg mice and dnNRSF Tg mice with a heterozygous GC-A background (dnNRSF Tg;GC-A$^{+/-}$ mice) grew normally until about 3 wk of age and started to die at ~4 wk of age (Fig. 1) (11). By contrast, ~80% of dnNRSF Tg;GC-A$^{-/-}$ mice died by 4 wk of age (by the time they were weaned), suggesting that GC-A is crucial for the survival of mice with dilated cardiomyopathy and lethal arrhythmia.

Diminished GC-A expression leads to deterioration of cardiac function in dnNRSF Tg mice. The perinatal lethality of the dnNRSF TG;GC-A$^{-/-}$ genotype made it difficult to assess cardiac function in these mice. We therefore used dnNRSF Tg;GC-A$^{+/-}$ mice, which expressed ~50% less GC-A mRNA than dnNRSF Tg mice, to evaluate the functional contribution of GC-A to the dnNRSF Tg heart (Fig. 2, *A* and *B*) (25). We initially compared the heart weight-to-body weight ratios in 8-wk-old WT, GC-A$^{+/-}$, dnNRSF Tg, and dnNRSF Tg;GC-A$^{+/-}$ mice. At that age, the cardiac structure and function of dnNRSF Tg mice were not yet disturbed (11). As shown in Fig. 2*C*, the heart weight-to-body weight ratios did not significantly differ among WT, dnNRSF Tg, and GC-A$^{+/-}$ mice but was significantly higher in dnNRSF Tg;GC-A$^{+/-}$ mice than in the other three groups. Moreover, subsequent echocardiography revealed dnNRSF Tg;GC-A$^{+/-}$ mice to have enlarged LV systolic and diastolic dimensions, increased LV mass, and reduced systolic function compared with dnNRSF Tg mice (Table 1). The hemodynamic parameters obtained through intracardiac catheterization showed significantly reduced LV systolic pressure and impaired dP/d*t* (Table 1). Thus impairment of GC-A signaling appears to degrade cardiac function in dnNRSF Tg mice.

Reducing GC-A promotes cardiac pathology in dnNRSF Tg mice. Histological analysis revealed additional effects of diminished GC-A expression on the structure of the dnNRSF Tg heart. The left ventricles were dilated to a greater extent in 8-wk-old dnNRSF Tg;GC-A$^{+/-}$ mice than in dnNRSF Tg or GC-A$^{+/-}$ mice (Fig. 3*A*). In addition, microscopic examination showed fibrosis to be more extensive in dnNRSF Tg;GC-A$^{+/-}$ mice than dnNRSF Tg mice, suggesting that endogenous ANP/BNP acts via GC-A to attenuate cardiac fibrosis in dnNRSF Tg hearts (Fig. 3*B*).

Finally, we assessed the mRNA expression of ANP, BNP, skeletal α-actin, and SERCA2, four marker genes used to evaluate cardiac pathology, and the mRNA expression of HCN2, HCN4, and CACNA1H, which we previously reported to be upregulated in dnNRSF Tg hearts (11). In that earlier study, we also observed that cardiac expression of ANP, BNP, and skeletal α-actin mRNA is upregulated in 8-wk-old dnNRSF Tg mice but that expression of SERCA2 mRNA is similar in 8-wk-old WT and dnNRSF Tg mice (11). In the present study, we found that the levels of ANP mRNA in dnNRSF Tg;GC-A$^{+/-}$ mice were even higher than in dnNRSF Tg hearts, whereas the levels of BNP mRNA were similar in dnNRSF Tg;GC-A$^{+/-}$ and dnNRSF Tg hearts (Fig. 4). Moreover, levels of skeletal α-actin mRNA were higher, whereas those of SERCA2 mRNA were significantly lower in dnNRSF Tg;GC-A$^{+/-}$ hearts than dnNRSF Tg hearts (Fig. 4). Taken together, these findings are consistent with the notion that reducing GC-A expression promotes pathological remodeling of dnNRSF Tg hearts. The cardiac expression of HCN2, HCN4, and CACNA1H mRNA did not significantly differ in dnNRSF Tg;GC-A$^{+/+}$ and dnNRSF Tg;GC-A$^{+/-}$ mice (Fig. 5).

DISCUSSION

Although it is well recognized that ventricular expression of both ANP and BNP is upregulated in hearts affected by dilated

Table 1. *Echocardiographic and hemodynamic analysis of 8-wk-old mice*

	GCA$^{+/+}$	GCA$^{+/-}$	dnNRSF Tg;GCA$^{+/+}$	dnNRSF Tg;GCA$^{+/-}$
Echocardiographic data	$n = 6$	$n = 4$	$n = 6$	$n = 4$
HR, beats/min	367.0±4.0	378.3±14.3	330.5±5.5	416.0±44.2
LVDd, mm	4.02±0.11	4.43±0.21	4.00±0.29	4.90±0.19*†
LVDs, mm	2.76±0.14	2.90±0.19	2.87±0.20	4.26±0.15*†‡
IVST, mm	0.66±0.04	0.63±0.03	0.65±0.03	0.58±0.05
PWT, mm	0.67±0.04	0.68±0.03	0.69±0.03	0.58±0.03
FS, %	32.8±1.9	34.0±4.5	27.9±1.5	12.8±1.5*†‡
EF, %	69.7±2.6	70.0±5.2	62.7±2.2	33.5±5.4*†‡
LVM, mg	90.2±8.1	104.2±1.8	89.3±3.0	116.6±11.7*†
Hemodynamic data	$n = 4$	$n = 5$	$n = 5$	$n = 5$
dP/dt_{max}, mmHg/s	4,865±201	5,005±283	4,757±325	3,747±202*†‡
dP/dt_{min}, mmHg/s	−4,935±218	−5,150±579	−4,756±237	−3,465±308*†‡
HR, min^{-1}	498±26.9	457±8.58	533±29.4	566±33.5‡
LVSP, mmHg	98.9±4.5	102.7±5.5	95.1±3.6	83.5±3.9*†
LVEDP, mmHg	2.25±0.56	3.15±0.38	2.36±0.69	2.73±0.85

Values are means ± SE; *n*, no. of mice. GC-A$^{+/+}$, guanylyl cyclase-A (GC-A)-sufficient; GC-A$^{+/-}$, GC-A heterozygous knockout mice; dnNRSF Tg, mice overexpressing a dominant-negative form of the transcriptional repressor neuron-restrictive silencer factor; HR, heart rate; LVDd, left ventricular end-diastolic dimension; LVDs, left ventricular end-systolic dimension; IVST, interventricular septal thickness; PWT, posterior wall thickness; FS, fractional shortening; EF, ejection fraction; LVM, left ventricular mass; dP/d*t*, first derivative of pressure; HR, heart rate; LVSP, left ventricular systolic pressure; LVEDP, left ventricular end-diastolic pressure. $P < 0.05$ vs. control wild-type mice (*), vs. dnNRSF Tg mice (†), and vs. GCA$^{+/-}$ mice (‡).

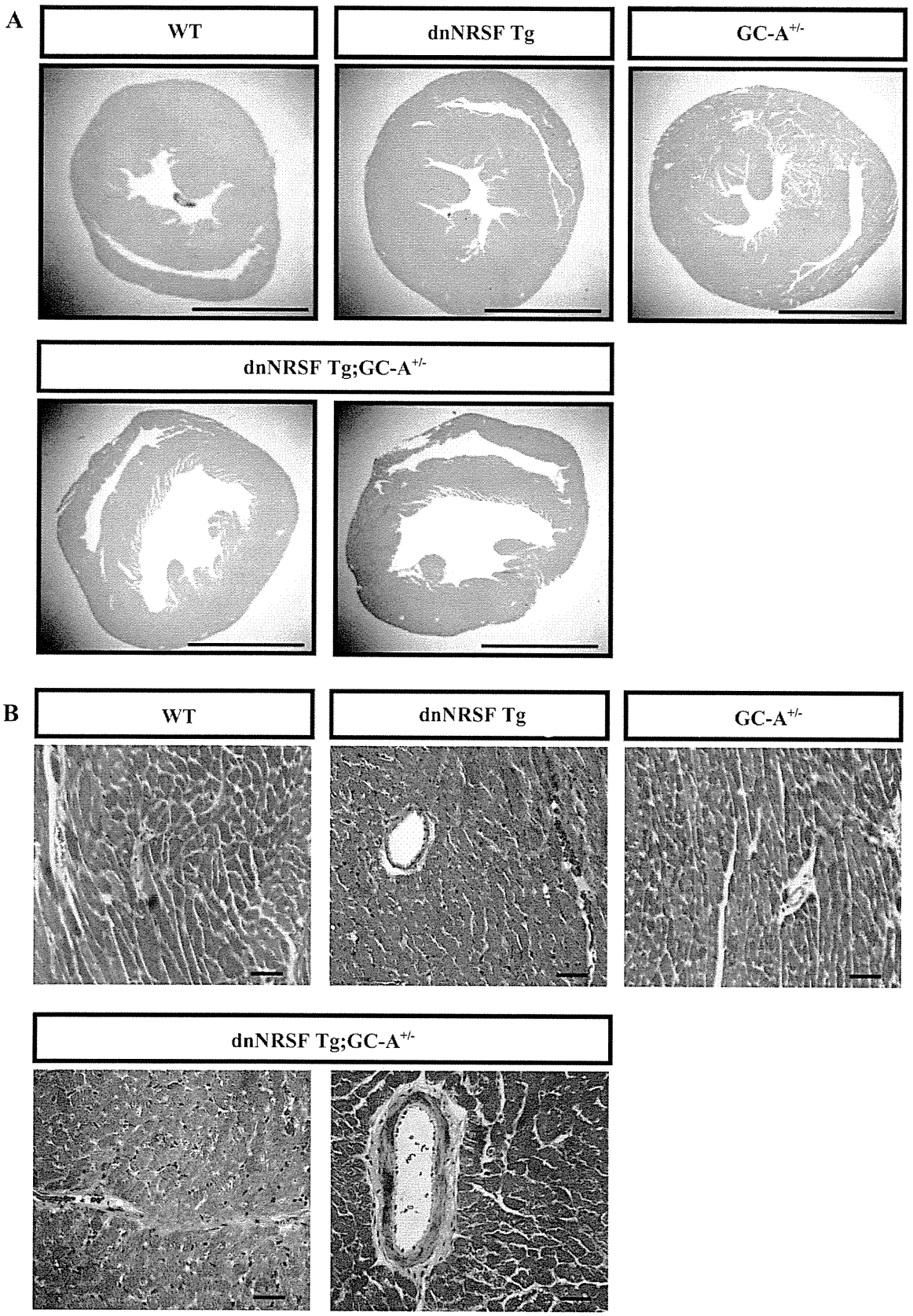

Fig. 3. Histological analysis. *A*: hematoxylin and eosin staining low-magnification photomicrographs showing the histology of wild-type, GC-A$^{+/-}$, dnNRSF Tg, and dnNRSF-Tg;GC-A$^{+/-}$ ventricles at 8 wk of age. Scale bars are 2.5 mm. *B*: Masson's trichrome staining showing fibrosis in sections from the left ventricles of wild-type, GC-A$^{+/-}$, dnNRSF Tg, and dnNRSF-Tg;GC-A$^{+/-}$ mice at 8 wk of age. Scale bars are 40 μm.

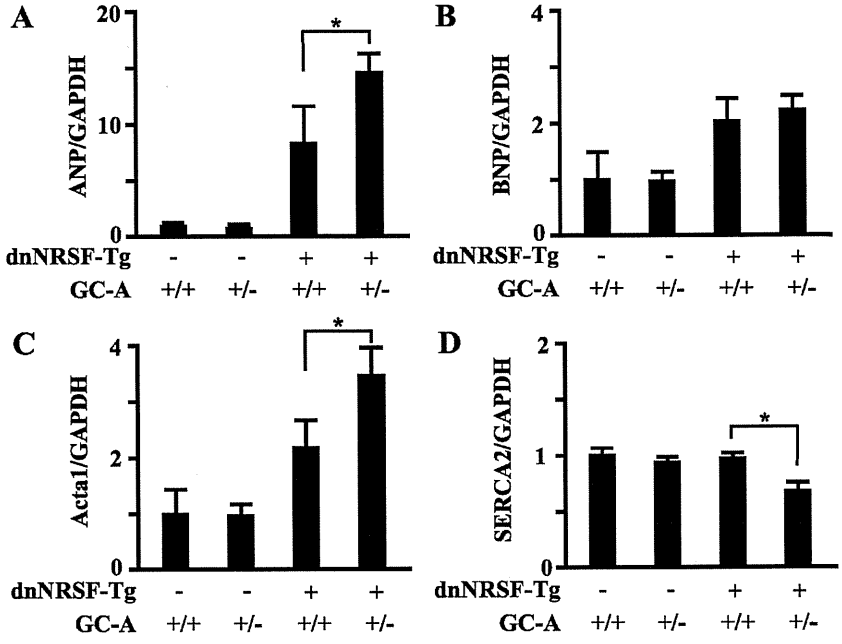

Fig. 4. Expression of atrial natriuretic peptide (ANP; *A*), brain natriuretic peptide (BNP; *B*), skeletal α-actin (*C*), and sarco(endo)plasmic reticulum Ca^{2+}-ATPase (SERCA2; *D*) mRNA in wild-type, GC-$A^{+/-}$, dnNRSF Tg, and dnNRSF-Tg;GC-$A^{+/-}$ mice. Samples (50 ng) of total RNA prepared from the ventricles of mice with the indicated genotypes were subjected to quantitative real-time PCR. Relative levels of ANP, BNP, skeletal α-actin, and SERCA2 mRNA, normalized to those of GAPDH mRNA, are shown. The levels in wild-type mice were assigned a value of 1. *$P < 0.05$.

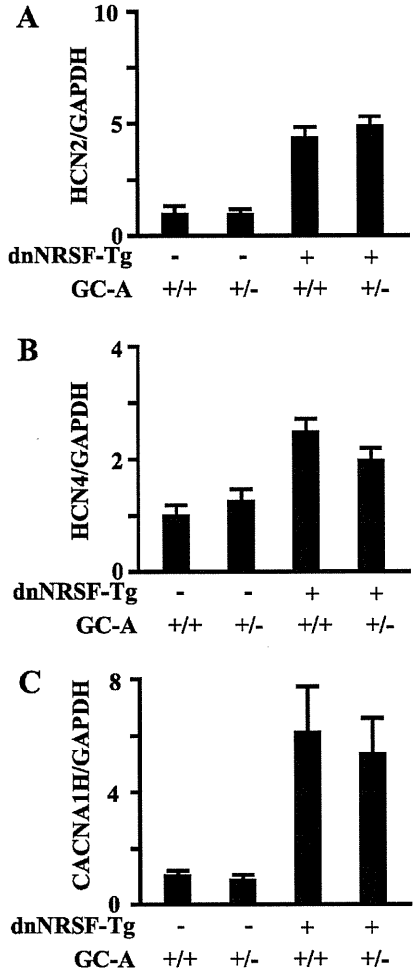

Fig. 5. Expression of HCN2 (*A*), HCN4 (*B*), and CACNA1H (*C*) mRNA in wild-type, GC-$A^{+/-}$, dnNRSF Tg, and dnNRSF-Tg;GC-$A^{+/-}$ mice. Relative levels of HCN2, HCN4, and CACNA1H mRNA, normalized to those of GAPDH mRNA, are shown. The levels in wild-type mice were assigned a value of 1.

cardiomyopathy (24), the effects of endogenous ANP/BNP during the development and progression of the ailment were not known. In the present study, we crossed dnNRSF Tg mice, a mouse model of dilated cardiomyopathy leading to sudden death, with GC-$A^{-/-}$ mice, which lack the receptor for ANP and BNP. Almost all dnNRSF Tg;GC-$A^{-/-}$ mice died within 4 wk after birth, whereas dnNRSF Tg;GC-$A^{+/+}$ mice lived at least 6 wk; dnNRSF Tg;GC-$A^{+/-}$ mice showed cardiomyopathic phenotypes that were more severe than dnNRSF Tg;GC-$A^{+/+}$. The results indicate that an insufficiency of GC-A accelerates the progression from latent to more evident cardiomyopathy in dnNRSF Tg mice, suggesting endogenous ANP/BNP exerts a protective effect against the progression of pathological cardiac remodeling and sudden death.

In healthy hearts, ANP is primarily secreted from the atrium, whereas BNP is primarily secreted from the ventricle, although small amounts of BNP are secreted from the atrium (18, 21, 23, 31). Ventricular expression of both ANP and BNP is upregulated under such pathological conditions as cardiac hypertrophy and heart failure, which makes plasma ANP/BNP levels a good prognostic indicator of clinical severity in a variety of cardiac diseases (21). Moreover, because improvement of cardiac function in response to medical and/or nonmedical therapy is accompanied by reductions in plasma ANP/BNP levels, they can serve as objective indicators with which to monitor the efficacy of therapy (30). As hormones, ANP and BNP exert diuretic, natriuretic, and vasorelaxant effects and counteract the effects of the renin-angiotensin-aldosterone and sympathetic nervous systems (21, 24, 25). In addition, they also act as paracrine factors, exerting antihypertrophic and antifibrotic effects in the heart (5, 9, 29). For these reasons, ANP and BNP are already being used clinically in patients with acute heart failure (4, 32). The roles played by endogenous ANP/BNP in the pathophysiology of heart failure had nonetheless remained unresolved. However, we recently showed that endogenous ANP/BNP is protective against acute heart failure and cardiac remodeling following experimental myocardial infarction in

mice (20). In the present study, moreover, we have shown that endogenous ANP/BNP also protects the heart against the progression of cardiac dysfunction in a mouse model of nonischemic dilated cardiomyopathy. Together, these two findings demonstrate that endogenous ANP/BNP protect against pathological ventricular remodeling, regardless of the etiology of the cardiomyopathy.

We previously showed that dnNRSF Tg;GC-A$^{+/+}$ mice grow normally until around 6 wk of age but then progress into cardiac dysfunction and die as a result of lethal arrhythmias some time later (11). The perinatal lethality of the dnNRSF Tg;GC-A$^{-/-}$ genotype would seem to indicate that endogenous ANP/BNP is able to protect dnNRSF Tg mice from sudden cardiac death, perhaps by exerting an antiarrhythmic effect. That said, we were unable to confirm that dnNRSF Tg;GC-A$^{-/-}$ mice die from lethal ventricular arrhythmias because of the technical difficulty of continuously collecting electrocardiography from perinatal mice. Blood pressures are elevated in GC-A$^{-/-}$ mice (14), which raises the possibility that increased blood pressure accelerates the progression of cardiac dysfunction in dnNRSF Tg;GC-A$^{-/-}$ mice. There is also a possibility that an as yet unidentified fundamental alteration caused by the GC-A-null background may have affected the phenotype. On the other hand, the idea that ANP/BNP exerts an antiarrhythmic effect is consistent with findings of an earlier report showing that older (12 mo of age) GC-A$^{-/-}$ mice have an increased susceptibility to ventricular arrhythmias (8). It also suggests the potential usefulness of ANP/BNP in the treatment of cardiomyopathies with a high susceptibility to arrhythmias. Indeed, ANP reportedly exerts a protective effect against arrhythmias induced by ischemia-reperfusion in dogs (28) and against those induced by proarrhythmic drugs in rabbits (6). The mechanism by which ANP/BNP might prevent arrhythmias remains unknown, although the recent report that sildenefil, a specific phosphodiesterase type 5 inhibitor, reduces the severity of arrhythmias during ischemia in dogs (19) suggests the effect is mediated by increasing cGMP levels via activation of GC-A. All of these data are suggestive of the therapeutic potential of ANP/BNP for the prevention of malignant arrhythmias in patients with heart failure or myocardial ischemia.

In conclusion, we have demonstrated that endogenous cardiac natriuretic peptides are able to markedly slow adverse cardiac remodeling during the progression of nonischemic cardiomyopathy toward sudden cardiac death. ANP and BNP are already being used to treat patients with acute heart failure. It is our hope that these findings begin to form the basis for novel and improved approaches to the treatment of patients with chronic heart failure and a high susceptibility to sudden cardiac death.

ACKNOWLEDGMENTS

We thank Okazaki and Kubo for excellent secretarial works.

GRANTS

This research was supported by a Grant-in-Aid for Scientific Research from the Japan Society for the Promotion of Science and grants from the Japanese Ministry of Health, Labor and Welfare, the Japan Heart Foundation/Pfizer Pharmaceuticals Inc. Grant on Cardiovascular Disease Research, the Japan Heart Foundation/Novartis Grant for Research Award on Molecular and Cellular Cardiology, the Mochida Memorial Foundation for Medical and Pharmaceutical Research, the Uehara Memorial Foundation, the Ichiro Kanehara Foundation, the Astellas Foundation for Research on Metabolic Disorders, the Mitsubishi Foundation, the Suzuken Memorial Foundation, the Takeda Medical Research Foundation, and the Kanae Foundation for the Promotion of Medical Science.

REFERENCES

1. **Abraham WT, Gilbert EM, Lowes BD, Minobe WA, Larrabee P, Roden RL, Dutcher D, Sederberg J, Lindenfeld JA, Wolfel EE, Shakar SF, Ferguson D, Volkman K, Linseman JV, Quaife RA, Robertson AD, Bristow MR.** Coordinate changes in Myosin heavy chain isoform gene expression are selectively associated with alterations in dilated cardiomyopathy phenotype. *Mol Med* 8: 750–760, 2002.
2. **Blaxall BC, Tschannen-Moran BM, Milano CA, Koch WJ.** Differential gene expression and genomic patient stratification following left ventricular assist device support. *J Am Coll Cardiol* 41: 1096–1106, 2003.
3. **Chien KR, Knowlton KU, Zhu H, Chien S.** Regulation of cardiac gene expression during myocardial growth and hypertrophy: molecular studies of an adaptive physiologic response. *FASEB J* 5: 3037–3046, 1991.
4. **Colucci WS, Elkayam U, Horton DP, Abraham WT, Bourge RC, Johnson AD, Wagoner LE, Givertz MM, Liang CS, Neibaur M, Haught WH, LeJemtel TH.** Intravenous nesiritide, a natriuretic peptide, in the treatment of decompensated congestive heart failure. *Nesiritide Study Group N Engl J Med* 343: 246–253, 2000.
5. **Fujisaki H, Ito H, Hirata Y, Tanaka M, Hata M, Lin M, Adachi S, Akimoto H, Marumo F, Hiroe M.** Natriuretic peptides inhibit angiotensin II-induced proliferation of rat cardiac fibroblasts by blocking endothelin-1 gene expression. *J Clin Invest* 96: 1059–1065, 1995.
6. **Inaba H, Hayami N, Ajiki K, Sugishita Y, Kunishima T, Yamagishi N, Yamagishi S, Murakawa Y.** Human atrial natriuretic peptide suppresses torsades de pointes in rabbits. *Circ J* 72: 820–824, 2008.
7. **Kawakami R, Saito Y, Kishimoto I, Harada M, Kuwahara K, Takahashi N, Nakagawa Y, Nakanishi M, Tanimoto K, Usami S, Yasuno S, Kinoshita H, Chusho H, Tamura N, Ogawa Y, Nakao K.** Overexpression of brain natriuretic peptide facilitates neutrophil infiltration and cardiac matrix metalloproteinase-9 expression after acute myocardial infarction. *Circulation* 110: 3306–3312, 2004.
8. **Kirchhof P, Fabritz L, Kilic A, Begrow F, Breithardt G, Kuhn M.** Ventricular arrhythmias, increased cardiac calmodulin kinase II expression, and altered repolarization kinetics in ANP receptor deficient mice. *J Mol Cell Cardiol* 36: 691–700, 2004.
9. **Knowles JW, Esposito G, Mao L, Hagaman JR, Fox JE, Smithies O, Rockman HA, Maeda N.** Pressure-independent enhancement of cardiac hypertrophy in natriuretic peptide receptor A-deficient mice. *J Clin Invest* 107: 975–984, 2001.
10. **Koller KJ, Goeddel DV.** Molecular biology of the natriuretic peptides and their receptors. *Circulation* 86: 1081–1088, 1992.
11. **Kuwahara K, Saito Y, Takano M, Arai Y, Yasuno S, Nakagawa Y, Takahashi N, Adachi Y, Takemura G, Horie M, Miyamoto Y, Morisaki T, Kuratomi S, Noma A, Fujiwara H, Yoshimasa Y, Kinoshita H, Kawakami R, Kishimoto I, Nakanishi M, Usami S, Saito Y, Harada M, Nakao K.** NRSF regulates the fetal cardiac gene program and maintains normal cardiac structure and function. *Embo J* 22: 6310–6321, 2003.
12. **Levy D, Kenchaiah S, Larson MG, Benjamin EJ, Kupka MJ, Ho KK, Murabito JM, Vasan RS.** Long-term trends in the incidence of and survival with heart failure. *N Engl J Med* 347: 1397–1402, 2002.
13. **Li Y, Kishimoto I, Saito Y, Harada M, Kuwahara K, Izumi T, Takahashi N, Kawakami R, Tanimoto K, Nakagawa Y, Nakanishi M, Adachi Y, Garbers DL, Fukamizu A, Nakao K.** Guanylyl cyclase-A inhibits angiotensin II type 1A receptor-mediated cardiac remodeling, an endogenous protective mechanism in the heart. *Circulation* 106: 1722–1728, 2002.
14. **Lopez MJ, Wong SK, Kishimoto I, Dubois S, Mach V, Friesen J, Garbers DL, Beuve A.** Salt-resistant hypertension in mice lacking the guanylyl cyclase-A receptor for atrial natriuretic peptide. *Nature* 378: 65–68, 1995.
15. **Lowes BD, Gilbert EM, Abraham WT, Minobe WA, Larrabee P, Ferguson D, Wolfel EE, Lindenfeld J, Tsvetkova T, Robertson AD, Quaife RA, Bristow MR.** Myocardial gene expression in dilated cardiomyopathy treated with beta-blocking agents. *N Engl J Med* 346: 1357–1365, 2002.
16. **Maisel A.** B-type natriuretic peptide levels: diagnostic and prognostic in congestive heart failure: what's next? *Circulation* 105: 2328–2331, 2002.
17. **McKinsey TA, Olson EN.** Toward transcriptional therapies for the failing heart: chemical screens to modulate genes. *J Clin Invest* 115: 538–546, 2005.

18. **Mukoyama M, Nakao K, Hosoda K, Suga S, Saito Y, Ogawa Y, Shirakami G, Jougasaki M, Obata K, Yasue H, Kambayashi Y, Inouge K, Imura H.** Brain natriuretic peptide as a novel cardiac hormone in humans Evidence for an exquisite dual natriuretic peptide system, atrial natriuretic peptide and brain natriuretic peptide. *J Clin Invest* 87: 1402–1412, 1991.
19. **Nagy O, Hajnal A, Parratt JR, Vegh A.** Sildenafil (Viagra) reduces arrhythmia severity during ischaemia 24 h after oral administration in dogs. *Br J Pharmacol* 141: 549–551, 2004.
20. **Nakanishi M, Saito Y, Kishimoto I, Harada M, Kuwahara K, Takahashi N, Kawakami R, Nakagawa Y, Tanimoto K, Yasuno S, Usami S, Li Y, Adachi Y, Fukamizu A, Garbers DL, Nakao K.** Role of natriuretic peptide receptor guanylyl cyclase-A in myocardial infarction evaluated using genetically engineered mice. *Hypertension* 46: 441–447, 2005.
21. **Nakao K, Itoh H, Saito Y, Mukoyama M, Ogawa Y.** The natriuretic peptide family. *Curr Opin Nephrol Hypertens* 5: 4–11, 1996.
22. **Nakao K, Ogawa Y, Suga S, Imura H.** Molecular biology and biochemistry of the natriuretic peptide system. II. Natriuretic peptide receptors. *J Hypertens* 10: 1111–1114, 1992.
23. **Ogawa Y, Nakao K, Mukoyama M, Hosoda K, Shirakami G, Arai H, Saito Y, Suga S, Jougasaki M, Imura H.** Natriuretic peptides as cardiac hormones in normotensive and spontaneously hypertensive rats. The ventricle is a major site of synthesis and secretion of brain natriuretic peptide. *Circ Res* 69: 491–500, 1991.
24. **Oliver PM, Fox JE, Kim R, Rockman HA, Kim HS, Reddick RL, Pandey KN, Milgram SL, Smithies O, Maeda N.** Hypertension, cardiac hypertrophy, and sudden death in mice lacking natriuretic peptide receptor A. *Proc Natl Acad Sci USA* 94: 14730–14735, 1997.
25. **Oliver PM, John SW, Purdy KE, Kim R, Maeda N, Goy MF, Smithies O.** Natriuretic peptide receptor 1 expression influences blood pressures of mice in a dose-dependent manner. *Proc Natl Acad Sci USA* 95: 2547–2551, 1998.
26. **Olson EN, Schneider MD.** Sizing up the heart: development redux in disease. *Genes Dev* 17: 1937–1956, 2003.
27. **Stanek B, Frey B, Hulsmann M, Berger R, Sturm B, Strametz-Juranek J, Bergler-Klein J, Moser P, Bojic A, Hartter E, Pacher R.** Prognostic evaluation of neurohumoral plasma levels before and during beta-blocker therapy in advanced left ventricular dysfunction. *J Am Coll Cardiol* 38: 436–442, 2001.
28. **Takata Y, Hirayama Y, Kiyomi S, Ogawa T, Iga K, Ishii T, Nagai Y, Ibukiyama C.** The beneficial effects of atrial natriuretic peptide on arrhythmias and myocardial high-energy phosphates after reperfusion. *Cardiovasc Res* 32: 286–293, 1996.
29. **Tamura N, Ogawa Y, Chusho H, Nakamura K, Nakao K, Suda M, Kasahara M, Hashimoto R, Katsuura G, Mukoyama M, Itoh H, Saito Y, Tanaka I, Otani H, Katsuki M.** Cardiac fibrosis in mice lacking brain natriuretic peptide. *Proc Natl Acad Sci USA* 97: 4239–4244, 2000.
30. **Troughton RW, Frampton CM, Yandle TG, Espiner EA, Nicholls MG, Richards AM.** Treatment of heart failure guided by plasma amino-terminal brain natriuretic peptide (N-BNP) concentrations. *Lancet* 355: 1126–1130, 2000.
31. **Yasue H, Yoshimura M, Sumida H, Kikuta K, Kugiyama K, Jougasaki M, Ogawa H, Okumura K, Mukoyama M, Nakao K.** Localization and mechanism of secretion of B-type natriuretic peptide in comparison with those of A-type natriuretic peptide in normal subjects and patients with heart failure. *Circulation* 90: 195–203, 1994.
32. **Yoshimura M, Yasue H, Ogawa H.** Pathophysiological significance and clinical application of ANP and BNP in patients with heart failure. *Can J Physiol Pharmacol* 79: 730–735, 2001.
33. **Yoshimura M, Yasue H, Okumura K, Ogawa H, Jougasaki M, Mukoyama M, Nakao K, Imura H.** Different secretion patterns of atrial natriuretic peptide and brain natriuretic peptide in patients with congestive heart failure. *Circulation* 87: 464–469, 1993.
34. **Zannad F, Briancon S, Juilliere Y, Mertes PM, Villemot JP, Alla F, Virion JM.** Incidence, clinical and etiologic features, and outcomes of advanced chronic heart failure: the EPICAL Study. Epidemiologie de l'Insuffisance Cardiaque Avancee en Lorraine. *J Am Coll Cardiol* 33: 734–742, 1999.

FEBS Letters 583 (2009) 2067–2070

ELSEVIER

FEBS Letters

journal homepage: www.FEBSLetters.org

Inhibition of hepatic damage and liver fibrosis by brain natriuretic peptide

Takuhiro Sonoyama, Naohisa Tamura *, Kazutoshi Miyashita, Kwijun Park, Naofumi Oyamada, Daisuke Taura, Megumi Inuzuka, Yasutomo Fukunaga, Masakatsu Sone, Kazuwa Nakao

Department of Medicine and Clinical Science, Kyoto University Graduate School of Medicine, 54 Shogoin-Kawahara-cho, Sakyo-ku, Kyoto 606-8507, Japan

ARTICLE INFO

Article history:
Received 15 January 2009
Revised 11 May 2009
Accepted 14 May 2009
Available online 20 May 2009

Edited by Veli-Pekka Lehto

Keywords:
Brain natriuretic peptide
Guanylyl cyclase-A
Carbon tetrachloride
Liver fibrosis
Hepatic stellate cell

ABSTRACT

Anti-fibrotic and organ protective effects of brain natriuretic peptide (BNP) have been reported. In this study, effects of BNP on liver fibrosis were examined in the carbon tetrachloride (CCl_4)-induced liver fibrosis model using BNP-transgenic (Tg) and wild-type (WT) mice. Twice-a-week intraperitoneal injections of CCl_4 for 8 weeks resulted in massive liver fibrosis, augmented transforming growth factor (TGF)-β_1 and type I procollagen α_1 chain (Col1a1) mRNA expression, and the hepatic stellate cell (HSC) activation in WT mice, all of which were significantly suppressed in Tg mice. These observations indicate that BNP inhibits liver fibrosis by attenuating the activation of HSCs.

1. Introduction

Natriuretic peptides (NPs) are a family of peptides, which consist of atrial, brain, and C-type NPs (ANP, BNP, and CNP, respectively) [1]. NPs' biological actions are mainly mediated by two NP receptors: guanylyl cyclase (GC)-A and GC-B [1]. NPs increase intracellular cGMP concentrations upon ligand binding. ANP and BNP are cardiac hormones produced mainly in the cardiac atria and ventricles, respectively, and play important roles to maintain cardiovascular homeostasis by activating GC-A [1]. CNP binds to GC-B, and the CNP/GC-B system takes part in the endochondral ossification and the vascular remodeling [1].

Carbon tetrachloride (CCl_4)-induced liver fibrosis is one of the most utilized animal models for liver fibrosis. CCl_4 selectively damage hepatocytes around central veins (centrilobular regions), which highly express cytochrome P450 2E1 (CYP2E1) that change CCl_4 into reactive oxygen species (ROS) [2]. Damaged hepatocytes recruit leukocytes and stimulate Kupffer cells to secrete several proinflammatory cytokines such as tumor necrosis factor-α, which activate hepatic stellate cells (HSCs). Transforming growth factor (TGF)-β_1 released from damaged hepatocytes also activates adjacent HSCs [3]. Activated HSCs become myofibroblast-like cells, which express α-smooth muscle actin (SMA), intensely proliferate, profoundly synthesize collagen, and produce profibrotic cytokines including TGF-β_1, leading to the development of liver fibrosis [3]. Also in non-alcoholic steatohepatitis (NASH) and alcoholic steatohepatitis, CYP2E1-derived ROS induce hepatocellular damage and HSC activation, leading to liver fibrosis [2,4].

While antifibrotic effects of CNP were shown in lungs and hearts of experimental animal models [5,6], we showed antifibrotic effects of BNP in the heart and kidneys [7,8]. In this study, we used BNP-transgenic (Tg) mice [9] in the CCl_4-induced liver fibrosis model to investigate effects of BNP on liver damage and fibrosis.

2. Materials and methods

2.1. Animals

Male wild-type (WT) C57BL/6 J mice (Shimizu Experimental Supplies, Kyoto, Japan) and male BNP-Tg mice of line 75 overexpressing BNP (8 weeks of age, 25–30 g of body weight) were used. The BNP-Tg mice harbor a transgene that expresses BNP under the control of the human serum amyloid P promoter, which is active in the liver after birth, and their plasma BNP concentrations were comparable to those in patients with severe congestive

Abbreviations: BNP, brain natriuretic peptide; CCl_4, carbon tetrachloride; Tg, transgenic; WT, wild-type; TGF, transforming growth factor; Col1a1, type I procollagen α_1 chain; HSC(s), hepatic stellate cell(s) NP, natriuretic peptide; ANP, atrial natriuretic peptide; CNP, C-type natriuretic peptide; GC, guanylyl cyclase; ROS, reactive oxygen species; CYP2E1, cytochrome P450 2E1; NASH, non-alcoholic steatohepatitis; SMA, smooth muscle actin; DMN, dimethylnitrosamine

* Corresponding author. Fax: +81 75 771 9452.
E-mail address: ntamura@kuhp.kyoto-u.ac.jp (N. Tamura).

0014-5793/$36.00
doi:10.1016/j.febslet.2009.05.025

heart failure [9]. Concentrations of BNP-like immunoreactivities in their livers were about 10-fold higher than their plasma BNP concentrations, but the majority of BNP-like immunoreactivities in their livers were proBNP, which is less active than mature peptide [9]. Mice were housed in a specified pathogen free facility with a 12-h light/dark cycle. Access to food and water was *ad libitum* throughout the study period. Mice were intraperitoneally injected with CCl_4 of 1 ml/kg body weight twice a week for 2–8 weeks to induce liver fibrosis. Mice were killed with the intraperitoneal injection of pentobarbital 3 days after the final CCl_4 injection, and livers were either fixed with 4% phosphate-buffered paraformaldehyde and embedded in paraffin for histological examination or immediately frozen in liquid nitrogen for the extraction of RNA. The experimental protocol of this study is approved by the Animal Research Committee, Kyoto University.

2.2. Histological analyses

Tissue sections were stained with hematoxylin and eosin or Sirius red to evaluate histological changes and collagen fiber deposition, respectively. To quantify the extent of fibrosis, percentages of Sirius red-positive pixels were measured in five randomly selected microscope fields at 40× magnification and averaged for each specimen by a technician, who did not know the genotype of each specimen. The sections were also subjected to immunohistochemistry with an antibody against mouse α-SMA (M0851, DAKO, Denmark), as described previously [10].

2.3. Extraction and analysis of RNA

Total RNA extracted from livers using an RNeasy Mini kit (Qiagen, Tokyo, Japan) was reverse-transcribed using a PrimeScript RT-PCR kit (Takara Bio, Otsu, Japan), and subjected to a real-time quantitative PCR using an ABI Prism 7300 Sequence Detection System (Applied Biosystems, Foster City, CA) with SYBR Premix Ex Taq (Takara Bio, Otsu, Japan) to evaluate mRNA levels of TGF-β_1, type I procollagen α1 chain (Col1a1), and α-SMA, according to the manufacturers' instructions. Levels of mRNA were normalized with those of a house keeping gene, β-actin. The primers used are shown in Supplementary Table 1.

2.4. Statistics

All values are expressed as means ± standard errors of the mean. Statistical differences in averages between two groups and among three or more groups were assessed by unpaired *t*-test and ANOVA, respectively.

3. Results and discussion

Before CCl_4 injections and after 2 weeks of repeated CCl_4 injections, hepatocellular damage and liver fibrosis were not evident both in WT and Tg mice (Fig. 1A and B). In WT mice, hepatocellular necrosis with inflammatory cell infiltration and fibrosis appeared in centrilobular regions after 4 weeks of CCl_4 injections (Fig. 1C), and hepatocellular necrosis was observed throughout the liver and septal fibrosis emerging from centrilobular regions formed central–central bridging necrosis after 8 weeks of CCl_4 injections (Fig. 1D). This is the typical time course of histological changes in this model [3], showing the model was adequately prepared in this study. In Tg mice, the extent of liver fibrosis was significantly suppressed compared with that of WT mice after 8 weeks of CCl_4 injections (Fig. 1D and E).

Hepatic TGF-β_1 and Col1a1 mRNA levels were not different between WT and Tg mice before CCl_4 injections (Fig. 2). After 2 weeks of CCl_4 injections, hepatic TGF-β_1 and Col1a1 mRNA levels tended to increase compared with those before CCl_4 injections in WT mice,

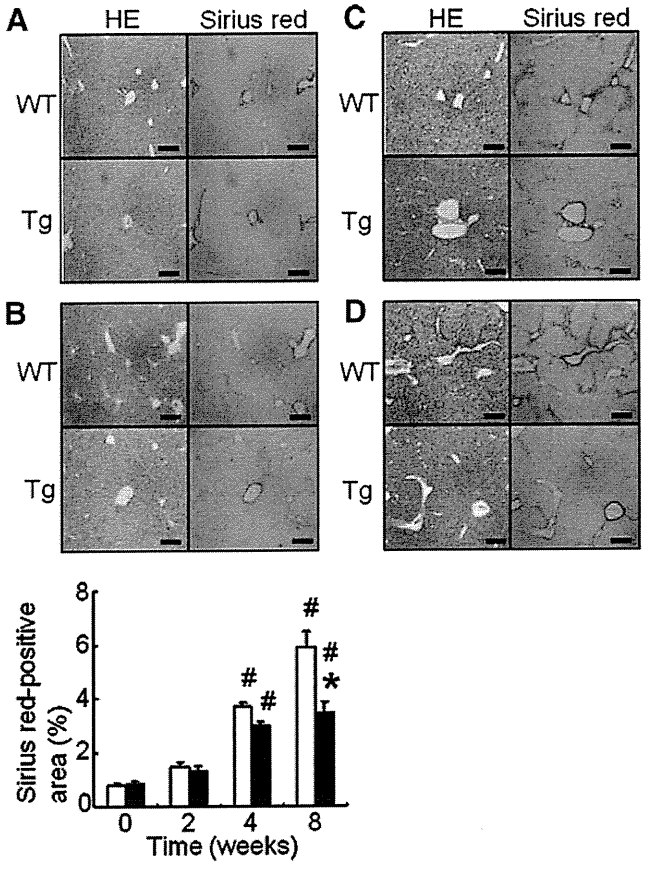

Fig. 1. Typical images of Hematoxylin and Eosin (HE) and Sirius red staining of livers from wild-type (WT) and BNP-transgenic (Tg) mice before CCl_4 injections (A), and after 2 (B), 4 (C), and 8 weeks of twice-a-week CCl_4 injections (D) are shown. Scale bars indicate 100 μm. Collagen fibrils are stained red by Sirius red. (E) The extent of liver fibrosis is quantified as the percentage of Sirius red-positive areas (before CCl_4 injections, $n = 5$ for each genotype; after 2, 4, and 8 weeks of CCl_4 injections, $n = 4$, 4, and 8 for each genotype, respectively). Data of WT and Tg mice are shown with open and closed columns, respectively. $^*P < 0.05$ vs. WT mice at each time point; $^\#P < 0.05$ vs. before CCl_4 injections in the same genotype by ANOVA.

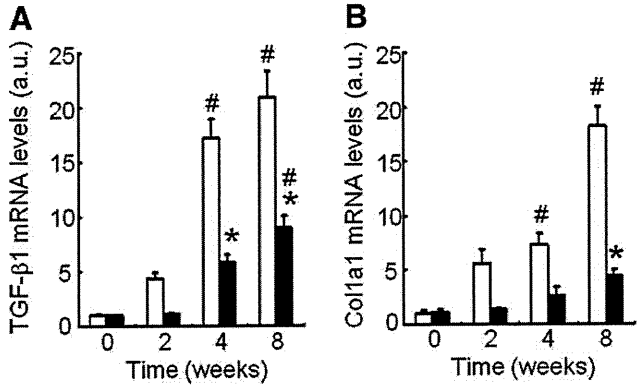

Fig. 2. Real-time quantitative PCR analysis of hepatic transforming growth factor (TGF)-β_1 (A) and type I procollagen α_1 chain (Col1a1) (B) mRNA levels in wild-type (WT, open columns) and BNP-transgenic (Tg, closed columns) mice before CCl_4 injections ($n = 5$ for each genotype) and after 2, 4, and 8 weeks of CCl_4 injections ($n = 4$, 4, and 8 for each genotype, respectively). The average of mRNA levels of each gene in WT livers before CCl_4 injections is set 1.0 arbitrary unit (a.u.). $^*P < 0.05$ vs. WT mice at each time point; $^\#P < 0.05$ vs. before CCl_4 injections in the same genotype by ANOVA.

while they remained similar to those before CCl_4 injections in Tg mice (Fig. 2). After 4 or 8 weeks of CCl_4 injections, hepatic TGF-β_1 and Col1a1 mRNA levels significantly increased compared with those before CCl_4 injections in WT mice (Fig. 2). Only TGF-β_1 mRNA levels were suppressed in Tg mice compared with those in WT mice after 4 weeks of CCl_4 injections, and both TGF-β_1 and Col1a1 mRNA levels were suppressed in Tg mice compared with those in WT mice after 8 weeks of CCl_4 injections (Fig. 2). We reported that BNP suppresses TGF-β_1 and Col1a1 mRNA levels and exerts anti-fibrotic and organ protective effects in the heart and kidneys [7,8]. This study added the liver to targets of those effects of BNP.

Alpha-SMA-positive cells, which are activated, myofibroblastic HSCs, were not detected in livers of WT and Tg mice before CCl_4 injections (Fig. 3A). After 8 weeks of CCl_4 injections, lots of α-SMA-positive cells were observed in regions of bridging necrosis in WT mice, but they were hardly seen in Tg mice (Fig. 1D and 3A). Hepatic α-SMA mRNA levels were attenuated in Tg mice compared with WT mice after 8 weeks of CCl_4 injections (Fig. 3B).

An *in vitro* study showed that activated human HSCs expressed GC-B without GC-A, suggesting that CNP has a potential to prevent HSCs' activation via GC-B and to counteract liver fibrosis [11]. On the contrary, it was reported that both quiescent and activated human HSCs expressed GC-A mRNA [13]. It was also reported that HSCs isolated from rats with CCl_4-induced cirrhosis expressed a higher number of ANP receptors compared with HSCs isolated from normal rats, indicating that *in vivo* activation of HSCs is associated with an up-regulation of ANP receptors [12]. GC-A mRNA expression was detected also in hepatocytes and Kupffer cells isolated from rat livers, and ANP could prevent ischemia-reperfusion injury of rat livers, which was caused by ROS generated by Kupffer cells, via GC-A [13]. During the course of our experiments, Ishigaki and colleagues reported that a continuously intravenous infusion of ANP could suppress dimethylnitrosamine (DMN)-induced liver damage and fibrosis by inhibiting HSC activation in rats [14]. It is speculated that an activation of GC-A can prevent liver fibrosis due to hepatocellular damage, because either an intravenous administration of ANP in rats or increased circulating BNP concentrations in Tg mice could prevent hepatocellular damage and liver fibrosis in different experimental models.

In the heart, signaling through GC-A inhibits angiotensin II type I receptor-mediated cardiac hypertrophy and fibrosis [15]. Olmesartan, an angiotensin II receptor blocker, reportedly inhibited liver fibrosis caused by NASH in mice [16]. An activation of GC-A might inhibit the renin–angiotensin system to protect the liver, but further studies will be needed to clarify the precise molecular mechanisms.

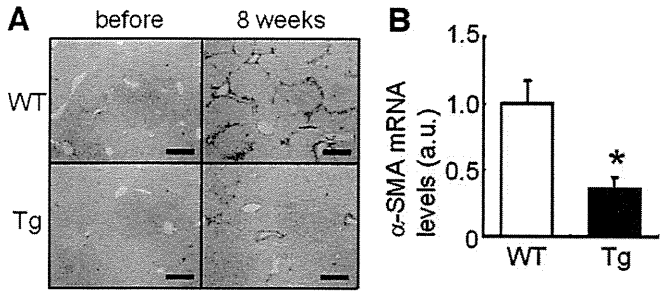

Fig. 3. Hapatic stellate cell activation in carbon tetrachloride-induced liver fibrosis. (A) Immunohistochemical detections of α-smooth muscle actin (SMA) in livers of wild-type (WT) and BNP-transgenic (Tg) mice before and after 8 weeks of CCl_4 injections. Scale bars indicate 100 μm. (B) Real-time quantitative PCR analysis of hepatic α-SMA mRNA levels in WT and Tg mice after 8 weeks of CCl_4 injections ($n = 8$ for each genotype). The average of mRNA levels in WT livers is set 1.0 arbitrary unit (a.u.). $^*P < 0.05$ vs. WT mice by unpaired *t*-test.

In conclusion, BNP could inhibit the CCl_4-induced liver fibrosis through the prevention of hepatocellular damage and HSC activation. Our findings may open up the possibility that BNP is therapeutically applicable for the prevention of liver fibrosis.

Acknowledgments

The authors thank Mr. Hirokazu Tsujimoto and Ms. Yoshie Fukuchi for technical assistance, Dr. Naoshi Nishida for expert opinions, and Mrs. Ayumi Ishida, Ms. Shiho Takada, and Ms. Aki Egami for secretarial assistance. This work was supported by the Takeda Science Foundation, the Takeda Medical Research Foundation, the Mochida Memorial Foundation for Medical and Pharmaceutical Research, the Cell Science Research Foundation, the Japan Smoking Foundation, a Grant-in-Aid for Scientific Research from the Ministry of Education, Culture, Sports, Science and Technology, and the Research Grant for Cardiovascular Diseases (19C-7 and 20C-3) from the Ministry of Health, Labour and Welfare.

Appendix A. Supplementary data

Supplementary data associated with this article can be found, in the online version, at doi:10.1016/j.febslet.2009.05.025.

References

[1] Tamura, N. and Garbers, D.L. (2004) Guanylyl cyclase receptors in: Encyclopedia of Endocrine Diseases (Martini, L. Ed.), vol. 2, pp. 415–421, Academic Press, San Diego.
[2] Chalasani, N., Gorski, J.C., Asghar, M.S., Asghar, A., Foresman, B., Hall, S.D. and Crabb, D.W. (2003) Hepatic cytochrome P450 2E1 activity in nondiabetic patients with nonalcoholic steatohepatitis. Hepatology 37, 544–550.
[3] Wallace, K., Burt, A.D. and Wright, M.C. (2008) Liver fibrosis. Biochem. J. 411, 1–18.
[4] Bradford, B.U., Kono, H., Isayama, F., Kosyk, O., Wheeler, M.D., Akiyama, T.E., Bleye, L., Krausz, K.W., Gonzalez, F.J., Koop, D.R. and Rusyn, I. (2005) Cytochrome P450 CYP2E1, but not nicotinamide adenine dinucleotide phosphate oxidase, is required for ethanol-induced oxidative DNA damage in rodent liver. Hepatology 41, 336–344.
[5] Murakami, S., Nagaya, N., Itoh, T., Fujii, T., Iwase, T., Hamada, K., Kimura, H. and Kangawa, K. (2004) C-type natriuretic peptide attenuates bleomycin-induced pulmonary fibrosis in mice. Am. J. Physiol. Lung Cell. Mol. Physiol. 287, L1172–7.
[6] Soeki, T., Kishimoto, I., Okumura, H., Tokudome, T., Horio, T., Mori, K. and Kangawa, K. (2005) C-type natriuretic peptide, a novel antifibrotic and antihypertrophic agent, prevents cardiac remodeling after myocardial infarction. J. Am. Coll. Cardiol. 45, 608–616.
[7] Tamura, N., Ogawa, Y., Chusho, H., Nakamura, K., Nakao, K., Suda, M., Kasahara, M., Hashimoto, R., Katsuura, G., Mukoyama, M., Itoh, H., Saito, Y., Tanaka, I., Otani, H. and Katsuki, M. (2000) Cardiac fibrosis in mice lacking brain natriuretic peptide. Proc. Natl. Acad. Sci. USA 97, 4239–4244.
[8] Suganami, T., Mukoyama, M., Sugawara, A., Mori, K., Nagae, T., Kasahara, M., Yahata, K., Makino, H., Fujinaga, Y., Ogawa, Y., Tanaka, I. and Nakao, K. (2001) Overexpression of brain natriuretic peptide in mice ameliorates immune-mediated renal injury. J. Am. Soc. Nephrol. 12, 2652–2663.
[9] Ogawa, Y., Itoh, H., Tamura, N., Suga, S., Yoshimasa, T., Uehira, M., Matsuda, S., Shiono, S., Nishimoto, H. and Nakao, K. (1994) Molecular cloning of the complementary DNA and gene that encode mouse brain natriuretic peptide and generation of transgenic mice that overexpress the brain natriuretic peptide gene. J. Clin. Invest. 93, 1911–1921.
[10] Sone, M., Itoh, H., Yamahara, K., Yamashita, JK., Yurugi-Kobayashi, T., Nonoguchi, A., Suzuki, Y., Chao, T.H., Sawada, N., Fukunaga, Y., Miyashita, K., Park, K., Oyamada, N., Sawada, N., Taura, D., Tamura, N., Kondo, Y., Nito, S., Suemori, H., Nakatsuji, N., Nishikawa, S. and Nakao, K. (2007) Pathway for differentiation of human embryonic stem cells to vascular cell components and their potential for vascular regeneration. Arterioscler. Thromb. Vasc. Biol. 27, 2127–2134.
[11] Tao, J., Mallat, A., Gallois, C., Belmadani, S., Méry, P.F., Nhieu, J.T., Pavoine, C. and Lotersztajn, S. (1999) Biological effects of C-type natriuretic peptide in human myofibroblastic hepatic stellate cells. J. Biol. Chem. 274, 23761–23769.
[12] Görbig, M.N., Ginès, P., Bataller, R., Nicolás, J.M., Garcia-Ramallo, E., Tobías, E., Titos, E., Rey, M.J., Clària, J., Arroyo, V. and Rodés, J. (1999) Atrial natriuretic peptide antagonizes endothelin-induced calcium increase and cell contraction in cultured human hepatic stellate cells. Hepatology 30, 501–509.
[13] Bilzer, M., Jaeschke, H., Vollmar, A.M., Paumgartner, G. and Gerbes, A.L. (1999) Prevention of Kupffer cell-induced oxidant injury in rat liver by atrial natriuretic peptide. Am. J. Physiol. 276, G1137–G1144.

[14] Ishigaki, N., Yamamoto, N., Jin, H., Uchida, K., Terai, S. and Sakaida, I. (2009) Continuous intravenous infusion of atrial natriuretic peptide (ANP) prevented liver fibrosis in rat. Biochem. Biophys. Res. Commun. 378, 354–359.
[15] Li, Y., Kishimoto, I., Saito, Y., Harada, M., Kuwahara, K., Izumi, T., Takahashi, N., Kawakami, R., Tanimoto, K., Nakagawa, Y., Nakanishi, M., Adachi, Y., Garbers, D.L., Fukamizu, A. and Nakao, K. (2002) Guanylyl cyclase-A inhibits angiotensin II type 1A receptor-mediated cardiac remodeling, an endogenous protective mechanism in the heart. Circulation 106, 1722–1728.
[16] Yamashita, T., Tokutomi, Y., Matsuba, S., Ichijo, H., Ogawa, H. and Kim-Mitsuyama, S. (2008) Olmesartan prevents cardiovascular injury and hepatic steatosis in obesity and diabetes, accompanied by apoptosis signal regulating kinase-1 inhibition. Hypertension 52, 573–580.

Urinary neutrophil gelatinase-associated lipocalin levels reflect damage to glomeruli, proximal tubules, and distal nephrons

Takashige Kuwabara[1], Kiyoshi Mori[1], Masashi Mukoyama[1], Masato Kasahara[1,2], Hideki Yokoi[1], Yoko Saito[1], Tetsuro Yoshioka[1], Yoshihisa Ogawa[1], Hirotaka Imamaki[1], Toru Kusakabe[1], Ken Ebihara[1], Mitsugu Omata[3], Noriko Satoh[4], Akira Sugawara[5], Jonathan Barasch[6] and Kazuwa Nakao[1]

[1]Department of Medicine and Clinical Science, Graduate School of Medicine, Kyoto University, Kyoto, Japan; [2]Division of Nephrology, Kobe City General Hospital, Kobe, Japan; [3]Biomedical Research Laboratories, Asubio Pharma, Osaka, Japan; [4]Clinical Research Institute for Endocrine Metabolic Diseases, National Hospital Organization, Kyoto Medical Center, Kyoto, Japan; [5]Department of Nephrology, Kyoto Medical Center, Kyoto, Japan and [6]Department of Medicine, College of Physicians and Surgeons, Columbia University, New York, New York, USA

Urinary neutrophil gelatinase-associated lipocalin (Ngal or lipocalin 2) is a very early and sensitive biomarker of kidney injury. Here we determined the origin and time course of Ngal appearance in several experimental and clinically relevant renal diseases. Urinary Ngal levels were found to be markedly increased in lipoatrophic- and streptozotocin-induced mouse models of diabetic nephropathy. In the latter mice, the angiotensin receptor blocker candesartan dramatically decreased urinary Ngal excretion. The reabsorption of Ngal by the proximal tubule was severely reduced in streptozotocin-induced diabetic mice, but upregulation of its mRNA and protein in the kidney was negligible, compared to those of control mice, suggesting that increased urinary Ngal was mainly due to impaired renal reabsorption. In the mouse model of unilateral ureteral obstruction, Ngal protein synthesis was dramatically increased in the dilated thick ascending limb of Henle and N was found in the urine present in the swollen pelvis of the ligated kidney. Five patients with nephrotic syndrome or interstitial nephritis had markedly elevated urinary Ngal levels at presentation, but these decreased in response to treatment. Our study shows that the urinary Ngal level may be useful for monitoring the status and treatment of diverse renal diseases reflecting defects in glomerular filtration barrier, proximal tubule reabsorption, and distal nephrons.

Kidney International (2009) **75**, 285–294; doi:10.1038/ki.2008.499; published online 1 October 2008

KEYWORDS: diabetic nephropathy; nephrotic syndrome; obstructive nephropathy; acute renal failure; albuminuria

Correspondence: *Kiyoshi Mori, Department of Medicine and Clinical Science, Graduate School of Medicine, Kyoto University, 54 Shogoin Kawahara-cho, Sakyo-ku, Kyoto 606-8507, Japan. E-mail: keyem@kuhp.kyoto-u.ac.jp*

Received 8 April 2008; revised 14 July 2008; accepted 12 August 2008; published online 1 October 2008

Neutrophil gelatinase-associated lipocalin (Ngal) is a differentiation inducer for epithelia in embryonic kidney, whose expression is dramatically increased in acute kidney injury (AKI).[1–5] Ngal exerts a spectrum of iron-dependent biological activities,[1–4,6] and administration of Ngal protein mitigates renal injury in mice, suggesting that functional consequence of Ngal upregulation is renoprotection.[2] Ngal mRNA levels in the kidney are increased as much as by 1000-fold during renal ischemia–reperfusion injury in mice.[2,7] Ngal protein starts to accumulate within a few hours in the blood and urine during AKI.[8–11] These characteristics of Ngal have made it a promising biomarker of AKI that is found in the blood and urine.[1,7,12–15] Furthermore, several studies reported that serum and urinary Ngal levels are elevated proportionally to the extent of renal damage in chronic kidney disease,[16,17] but the source and the time course of urinary Ngal concentrations are largely unknown. In this study, we investigated urinary Ngal levels in four types of renal damage caused by distinct mechanism: nephrotic syndrome caused by glomerular disorders, diabetic nephropathy, obstructive nephropathy, and interstitial nephritis. We also examined whether measurement of urinary Ngal is useful for the monitoring of renal damage in mice or humans during the treatment course.

RESULTS

Urinary Ngal excretion is proportional to albumin excretion in mouse models of diabetic nephropathy

As a model of diabetic nephropathy, we first examined urinary Ngal concentrations in A-ZIP/F-1 transgenic mice, which are characterized with lipoatrophic diabetes, fatty liver, hyperlipidemia, severe insulin resistance, and massive proteinuria.[18–20] Urinary Ngal excretion in A-ZIP/F-1 mice at 10 months of age was much larger than that in control FVB/N mice (Figure 1). By Western blot, we observed 30 and 25 kDa bands with Ngal immunoreactivity, and the larger band was found only in the urine from A-ZIP/F-1 mice and

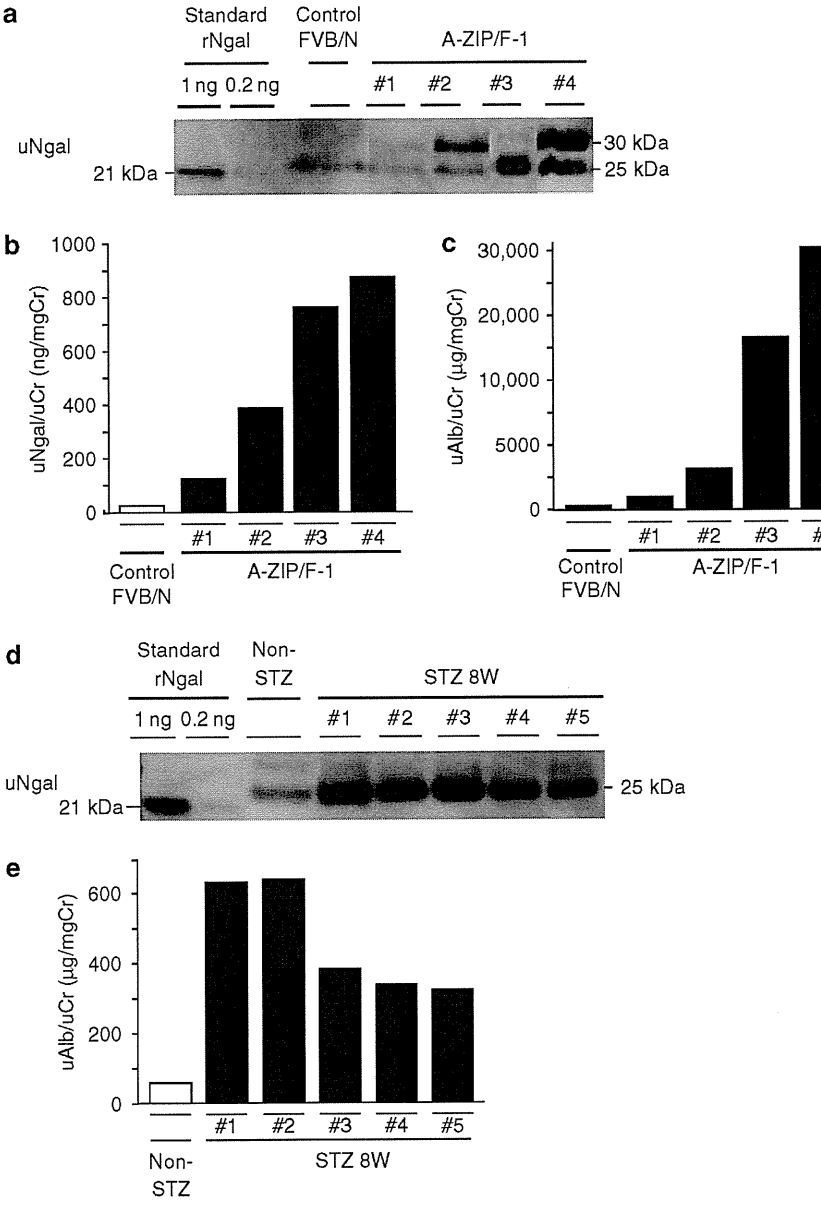

Figure 1 | Urinary Ngal and albumin excretion in two models of diabetic nephropathy. (**a–c**) A-ZIP/F-1 diabetic mice at 10 months of age and (**d**, **e**) diabetic mice at 8 weeks after streptozotocin (STZ) injection. (**a**, **d**) Western blot of urine (25 μl each) in individual mice and (**b**, **c**, **e**) urinary levels of Ngal and albumin (Alb) normalized by creatinine (Cr) are shown. (**b**) A-ZIP/F-1 mice, including no. 1, excreted much larger volumes of urine than control FVB/N mice. In three control FVB/N mice, mean urinary Ngal/Cr ratio (± s.e.) was 42 ± 24 ng per mgCr. uNgal, urinary Ngal; rNgal, recombinant Ngal.

not in the urine or tissues from normal, diabetic, or obstructed kidneys of mice with C57BL/6 background (see below). The larger protein may have heavier glycosylation than the smaller protein.[21] When the amounts of two proteins were added, mice with larger urinary Ngal levels tended to have larger urinary albumin levels.

Next, we studied streptozotocin (STZ)-induced diabetes, which manifests with insulin deficiency and microalbuminuria. In STZ mice, urinary albumin excretion increased gradually and, after 8 weeks, reached 7.8-fold of the level before STZ injection (Figure 2). On the other hand, urinary Ngal levels were elevated by 77-fold at 8 weeks. The extent of Ngal and albumin excretion was highly variable among different mice, but urinary albumin levels and log transformation of Ngal levels showed a close linear correlation throughout the course of 12-week observation period.

Elevation of urinary Ngal excretion in STZ mice is not caused by renal synthesis but by reabsorption defect, and treatment with angiotensin receptor blocker reduces urinary Ngal levels

To examine whether local expression of Ngal is increased in STZ mouse kidneys, we studied expression levels of Ngal protein in the whole kidney preparation of STZ and non-STZ control mice and found no significant difference at 8 weeks

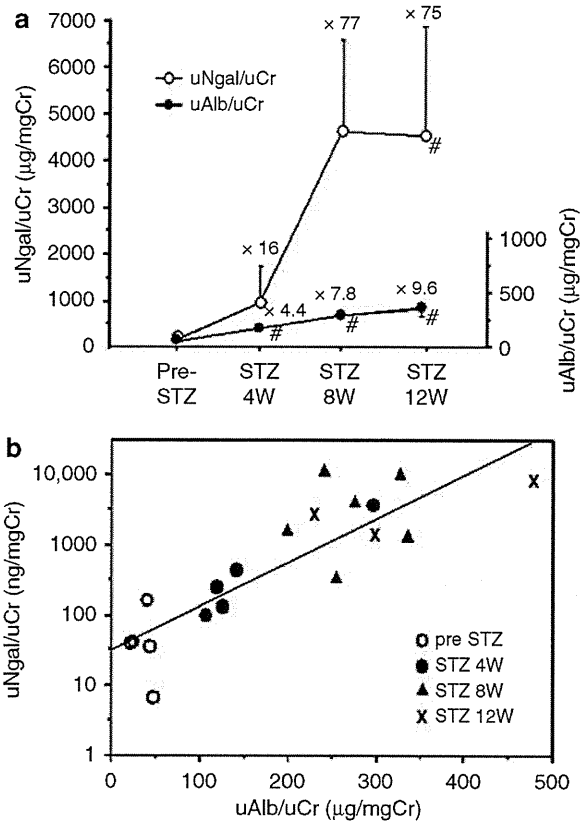

Figure 2 | Time course and correlation of urinary Ngal and albumin excretion in streptozotocin (STZ)-induced diabetic mice. (**a**) Urinary Ngal (uNgal) and albumin (uAlb) levels normalized by urinary creatinine (uCr) were examined before and at 4, 8, and 12 weeks after STZ injection (mean ± s.e.). #, $P<0.05$ versus pre-STZ. Elevation of urinary Ngal levels was significant at 4, 8, and 12 weeks if analyzed after log transformation. (**b**) Correlation between uNgal/uCr and uAlb/uCr; $r=0.86$, $P<0.001$, $n=19$.

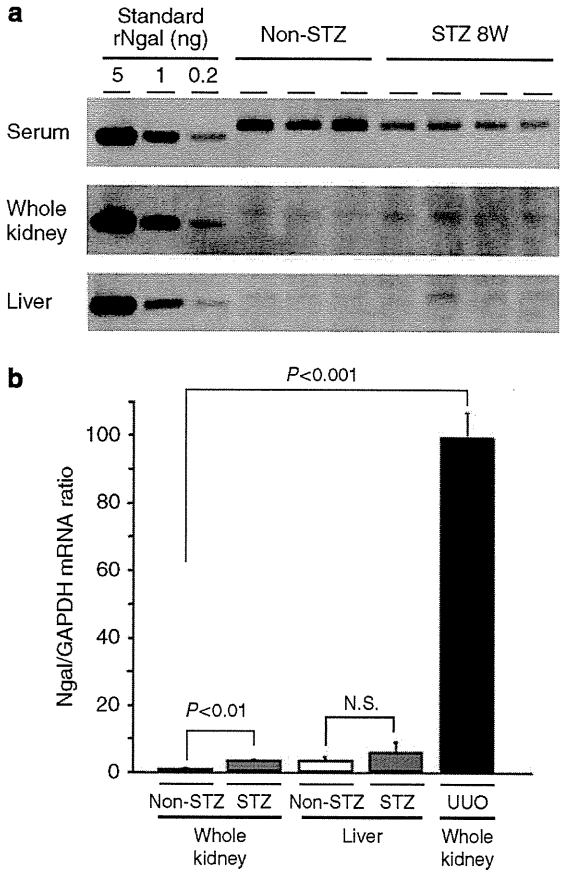

Figure 3 | Ngal protein and mRNA expression in the serum, kidney, and liver of STZ mice. (**a**) Western blot of serum, whole kidney, and liver at 8 weeks after induction of diabetes. Mice without STZ injection served as control (non-STZ). Equal amounts of serum (15 μl) and protein (30 μg) of whole kidney and liver were separated by electrophoresis; rNgal, recombinant Ngal. (**b**) Ngal mRNA expression levels were measured using real-time PCR and normalized by GAPDH expression ($n=4$). The mean Ngal/GAPDH level in non-STZ whole kidney was arbitrarily defined as 1.0. The whole kidneys at 1 day after unilateral ureteral obstruction (UUO) were also examined as a positive control. NS, not significant.

after STZ treatment (Figure 3). We did not find significant alteration of Ngal protein expression in the livers, either. Of note, serum Ngal levels in STZ mice were significantly lower than those in non-STZ mice (23 ± 5 versus 111 ± 22 ng/ml, $n=3$–4, $P<0.01$). We measured Ngal mRNA expression levels in the kidneys and livers of STZ mice, but they were increased only marginally compared to control mice. As a positive control, Ngal mRNA expression was increased by 100-fold in obstructed kidneys after 1 day of ureter ligation ($P<0.001$). These findings suggested that dramatic (nearly 80-fold) increase of urinary Ngal excretion in STZ mice cannot be explained by augmentation of Ngal protein synthesis in the kidney, and led us to investigate tubular reabsorption of Ngal. Injection of histidine-tagged or Alexa Fluor 546-labeled Ngal (21 kDa in size) in the peritoneum of non-STZ mice resulted in glomerular filtration and efficient reabsorption of Ngal at the proximal tubules from the apical side, thus no exogenous Ngal was detected in the urine (Figure 4). In STZ mice, on the other hand, substantial amount of exogenous Ngal was excreted in the urine and reabsorption of labeled Ngal was reduced by 47% ($P<0.01$).

As treatment of diabetic nephropathy with angiotensin receptor blocker (ARB) reduces proteinuria and ameliorates renal injury,[22] we gave the ARB candesartan to STZ mice through drinking water at 10 mg/kg/day (Figure 5). After 1 week, urinary albumin levels were decreased by 14% ($P<0.05$) and urinary Ngal levels were decreased by 77% ($P<0.05$). Serum Ngal levels were not altered by candesartan (20 ± 6 ng/ml). The dose of candesartan used was a subdepressor dose, and did not significantly affect body weights, blood glucose, urea nitrogen and creatinine levels (Table 1). Through these findings, we conclude that increased urinary Ngal excretion in STZ mice was caused mainly by reabsorption defect and treatment with candesartan partially normalized urinary Ngal levels.

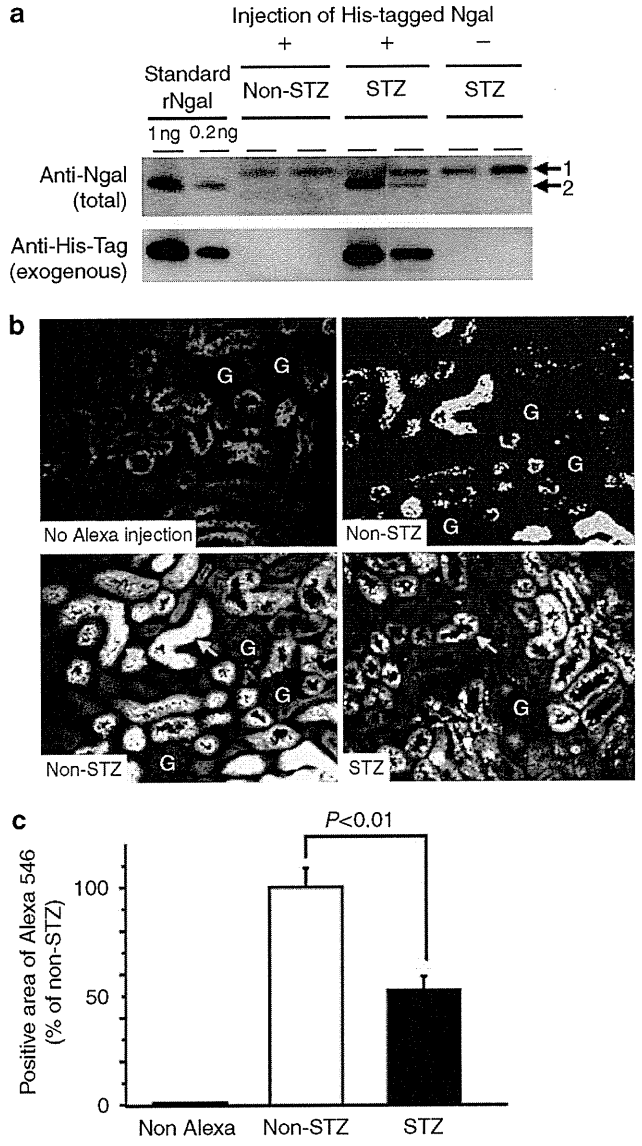

Figure 4 | Urinary excretion and tubular reabsorption of exogenously administered Ngal in STZ mice. (**a**) Western blot of urinary Ngal detected either with anti-Ngal or with anti-His-tag antibody at 8 weeks after induction of diabetes. Urine samples were collected for 12 h after His-tagged Ngal injection (i.p.) and 25 μl aliquots of them were separated by electrophoresis. Of note, STZ mice excreted much more diluted urine compared to non-STZ control mice. 1, endogenous Ngal (25 kDa, glycosylated); 2, His-tagged Ngal (21 kDa, unglycosylated). (**b**) Alexa Fluor 546-labeled Ngal was injected into STZ mice and kidneys were examined 30 min later. Arrows indicate Ngal protein distribution (in orange), which was homogeneous in non-STZ but was irregular and sparse in STZ mice. Top right panel shows selected area (in green) of positive fluorescence by computer software. G, glomeruli. Magnification, × 20. (**c**) Quantitation of exogenous Ngal uptake in kidneys of STZ and non-STZ mice ($n = 4$).

Urinary Ngal levels are highly elevated in human cases of nephrotic syndrome and are decreased in response to treatment

As cases of glomerular disorders with nephrotic syndrome, we investigated the clinical courses and changes in serum and urinary Ngal levels in human subjects. Case 1 was a 68-year-old woman with biopsy-proven minimal change disease. She had nephrotic range proteinuria (14 g/day) and gained body weight by 15 kg (from 62 to 77 kg) within 3 weeks. She was treated with i.v. steroid pulse (methyl prednisolone 1 g × 3 days), followed with oral prednisolone (beginning with 35 mg/day), and with three courses of hemodialysis on days 8, 9, and 12 after admission (Figure 6). Her proteinuria, edema, and azotemia resolved gradually. Concomitantly, urinary and serum Ngal levels decreased during the treatment, but reduction was much faster for urinary Ngal levels. There was a temporal elevation of urinary Ngal levels on day 21, which might reflect the reappearance of oligouria or proteinuria.

Case 2 was a 26-year-old woman, who was diagnosed to have membranous-type lupus nephritis (ISN/RPS class V). She was treated with two courses of i.v. steroid pulse, followed with oral prednisolone (Figure 6). Her urinary levels of protein and Ngal were decreased sharply within 17 days.

Case 3 was a 55-year-old woman with clinically diagnosed lupus nephritis (no biopsy). She had been treated with two courses of i.v. steroid pulse (1 g × 3 days) and oral prednisolone had been tapered from 50 to 35 mg/day, before changing the hospitals to ours. She was given i.v. cyclophosphamide pulse (0.4 g, once, 6 days after admission) and the immunosuppressant mizoribine (Asahi Kasei Pharma, Osaka, Japan; 100 mg/day). Urinary excretion of protein and Ngal decreased slowly (Supplementary Figure S1). Serum creatinine levels were constant throughout the course (0.4–0.5 mg/100 ml).

Case 4 was a 69-year-old man, who suffered from rapidly progressing, crescentic glomerulonephritis accompanied with moderate tubulointerstitial damage. His serum contained myeloperoxidase-type antineutrophil cytoplasmic antibody (MPO-ANCA, 138 EU). The maximum serum creatinine level was 5.6 mg/100 ml, and the proteinuria and azotemia responded slowly to treatment containing oral and i.v. steroid and i.v. cyclophosphamide (Supplementary Figure S1). Macrohematuria was observed, peaking at 5 days after cyclophosphamide administration. After 10 months, he showed signs of recurrence which were worsening in proteinuria, hematuria, azotemia, and MPO-ANCA titer (from <10 to 37 EU). We observed reelevation of urinary Ngal levels during acute worsening of nephritis. Cyclosporine A (75 mg/day before breakfast) was added at 13 months, which appeared to support reduction of above mentioned signs.

To understand renal localization of Ngal protein in nephrotic patients, we carried out immunofluorescence study of renal biopsy samples and found close colocalization of signals of Ngal and albumin at the apical side of tubules. The results for case 1 are shown in Figure 7. These findings are consistent with those in animal experiments shown above (Figure 4), indicating highly active reabsorption of Ngal from glomerular filtrate.

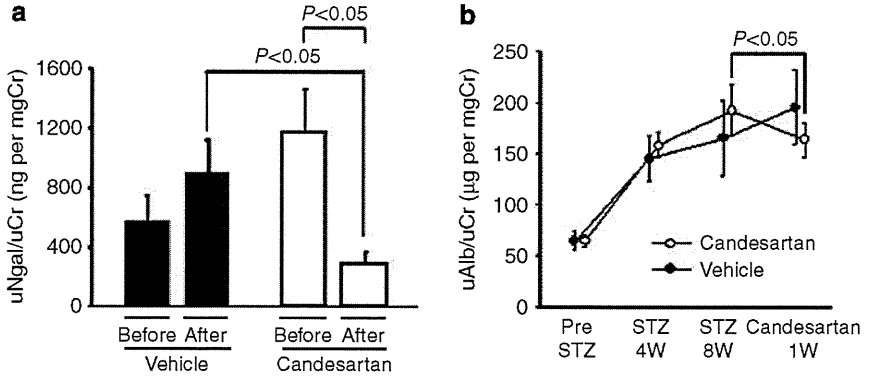

Figure 5 | Reduction of urinary Ngal and albumin excretion by candesartan in STZ mice. (**a**) Urinary Ngal (uNgal) and (**b**) albumin (uAlb) levels at 4 and 8 weeks after STZ injection and after one more week with candesartan (10 mg/kg/day, orally) or vehicle treatment ($n = 4$).

Table 1 | Blood glucose, urea nitrogen, creatinine levels, body weight, and blood pressure in STZ diabetic mice before and after candesartan treatment

	Vehicle		Candesartan	
	Before	After	Before	After
Blood glucose (mg/100 ml)	598 ± 2	593 ± 6	600 ± 3	591 ± 5
HbA1c (%)	11.7 ± 0.5	ND	12.5 ± 0.2	ND
Blood urea nitrogen (mg/100 ml)	ND	50 ± 2	ND	54 ± 1
Serum creatinine (mg/100 ml)	ND	0.13 ± 0.01	ND	0.11 ± 0.01
Body weight (g)	23.8 ± 0.9	23.5 ± 0.7	22.4 ± 0.5	22.8 ± 0.5
Systolic blood pressure (mm Hg)	104 ± 2	105 ± 0.9	103 ± 1	100 ± 1
Diastolic blood pressure (mm Hg)	55 ± 2	56 ± 1	50 ± 1	49 ± 2

Treatment with candesartan did not significantly alter these parameters. Blood urea nitrogen and serum creatinine levels in non-STZ control mice were 23 ± 3 and 0.09 ± 0.02 mg/100 ml, respectively. Blood was drawn when mice were fed *ad libitum*. ND, not determined.

In mice with obstructive nephropathy, Ngal protein is specifically located in the distal nephrons in the obstructed side by local synthesis, whereas it is confined to the proximal tubules in the contralateral side of the kidneys by reabsorption

As a model of post-renal kidney injury, we investigated mice with unilateral ureteral obstruction (UUO), in which distal nephrons are primarily affected, and studied the changes of Ngal protein levels in the obstructed and nonobstructed sides of the kidneys, serum, and urine (Figures 7 and 8). We also determined the renal distribution of Ngal by immunohistochemistry along with nephron segment markers: aquaporin (AQP) 1 for proximal tubules, Tamm-Horsfall protein (THP) for thick ascending limbs of Henle, and AQP 2 for collecting ducts (Figure 7; Figures S2–S4). In the UUO kidneys, after 1 day of ureter ligation, Ngal protein was expressed exclusively in thick ascending limbs of Henle, which was also expressing THP and was prominently dilated, suggesting that Ngal was synthesized in damaged epithelia. By striking contrast, in the contralateral kidneys, Ngal protein was confined to the apical side of aquaporin 1^+ proximal tubules. Ngal protein levels in the obstructed kidneys and in the urine from the dilated pelvis were continuously elevated for 2 weeks, whereas those in the nonobstructed kidneys and in the serum peaked at day 1 and decreased gradually. A smaller (17 kDa) fragment detected in the kidneys (but not in the urine and serum) using polyclonal anti-Ngal antibody may have been generated by lysosomal proteolysis of Ngal in the tubules.[2] Ngal mRNA expression was elevated by 100-fold in the obstructed kidneys (Figure 3), but it was only elevated by threefold in the contralateral kidneys at day 1 (data not shown). These findings indicate that Ngal was synthesized *de novo* in distal nephrons of obstructed kidneys, although it was highly but transiently accumulated in the serum, filtrated and reabsorbed in the contralateral kidneys.

In a case with interstitial nephritis, urinary Ngal levels decreased more rapidly than classic markers of tubular injury

Next, we investigated whether urinary Ngal is useful for evaluation of renal disorder with low-level proteinuria. Case 5 was a 25-year-old man, who was admitted to our hospital, presenting with general malaise, proteinuria (0.4 g/day), renal glucosuria and mild azotemia. He had taken an over-the-counter cold medicine 6 weeks earlier, and was positive in lymphocyte stimulation test for the drug. Renal biopsy revealed subacute interstitial nephritis with minor glomerular lesions. His signs and symptoms resolved by oral and i.v. prednisolone treatment. Table 2 and Figure S5 summarize the clinical course and changes in urinary biomarkers. The time to 50% reduction of urinary markers was in the order of Ngal $\leqslant$ (total) protein $<\alpha$1- and β2-microglobulins (classic markers of tubular proteinuria)

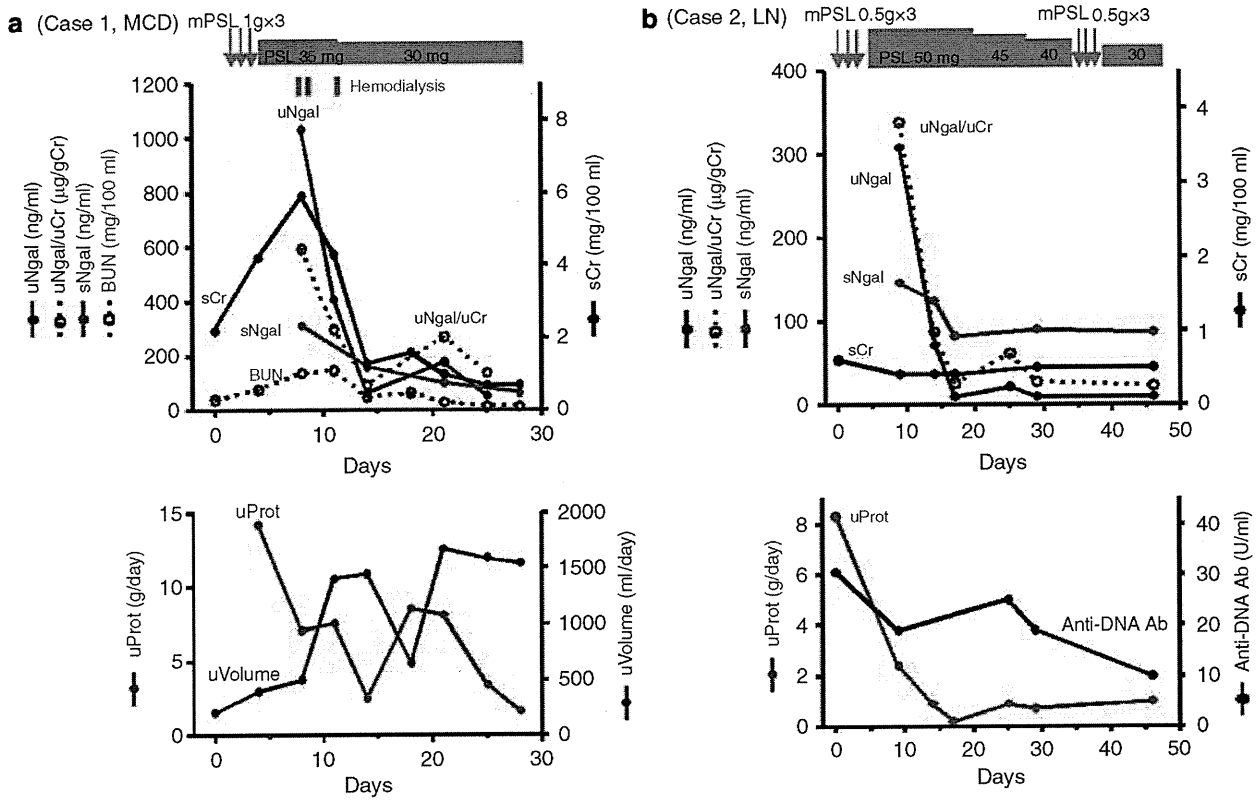

Figure 6 | Clinical course of 2 cases with nephrotic syndrome. (**a**) minimal change disease (case 1, MCD) and (**b**) lupus nephritis (case 2, LN). mPSL, methyl prednisolone; PSL, prednisolone; uProt, urinary protein excretion; sNgal, serum Ngal; uNgal, urinary Ngal; BUN, blood urea nitrogen; sCr, serum creatinine; uNgal/uCr, urinary Ngal normalized by urinary creatinine; Ab, antibody.

<*N*-acetyl-β-D-glucosaminidase. The fold-change during treatment was also largest in urinary Ngal, suggesting that urinary Ngal may be useful in monitoring the activity of nonglomerular renal disorders.

DISCUSSION

In the present study, we investigated urinary Ngal concentrations in patients with nephrotic syndrome (caused by acute and severe glomerular disorders) and interstitial nephritis and in mouse models of diabetic or obstructive nephropathy and found that the levels were unequivocally elevated (over 10-fold of control). In diabetic mice induced by STZ (as a model of slowly progressive chronic kidney disease), urinary Ngal appeared to derive mostly from impaired reabsorption in proximal tubules. In obstructed kidneys (as a model of post-renal AKI), Ngal was highly expressed in distal nephrons and accumulated in the urine collected from the pelvis. Therefore, STZ-diabetic and obstructed kidneys are the two extreme examples in which the primary source of urinary Ngal is glomerular filtrate and renal synthesis, respectively. In human renal disorders, urinary Ngal should be a mixture of these two major components. These findings indicate that in a variety of kidney diseases, urinary Ngal is a biomarker that can reflect damage in glomeruli, proximal tubules and distal nephrons.

Cross-sectional studies published so far have elucidated that urinary Ngal levels show certain correlation with urinary protein levels.[16,23] To our knowledge, this is the first human report to show very rapid and simultaneous reduction of urinary Ngal and protein concentrations by medical intervention. Surprisingly, the time course of urinary Ngal levels was associated to that of urinary protein levels not only in diabetic nephropathy and minimal change disease but also in crescentic glomerulonephritis and interstitial nephritis. In the latter disorders, treatment with steroid and immunosuppressant may have ameliorated Ngal reabsorption impairment and epithelial Ngal synthesis at the same time. The present findings suggest that urinary Ngal may be useful in the monitoring of disease activity and treatment efficacy. Of note, we cannot overgeneralize the findings in this study to all renal disorders, especially because we did not examine patients with severe, acute tubular necrosis, for instance, caused by renal ischemia or nephrotoxins (in which Ngal is abundantly synthesized by renal epithelia).[2]

In diabetic nephropathy, albumin excretion is increased by leakage from glomerular filtration barrier.[24] On the other hand, a number of reports elucidated the involvement of tubular dysfunction as a cause of albuminuria.[24–27] The size of Ngal protein (25 kDa) is smaller than albumin and, in normal conditions, Ngal is rapidly filtered by glomeruli and

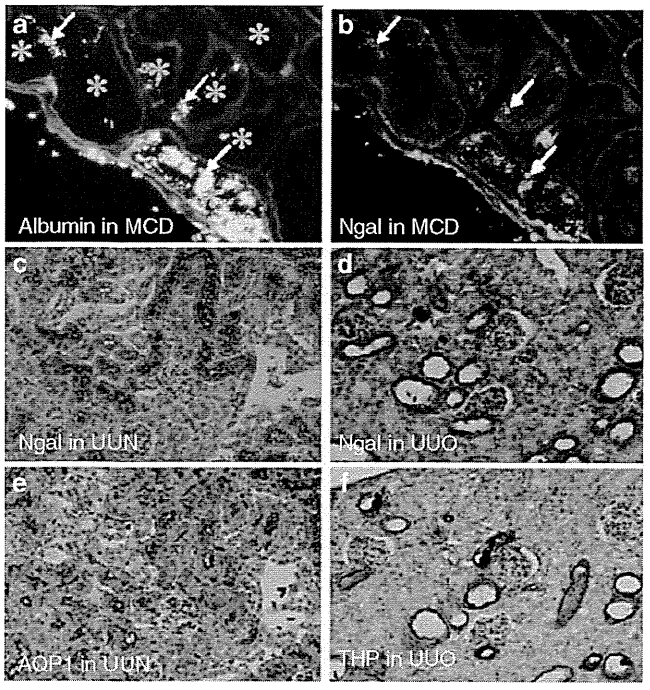

Figure 7 | Localization of Ngal protein expression in human and mouse kidneys. Immunofluorescence of (**a**, green) albumin and (**b**, red) Ngal in a patient with minimal change disease (MCD, magnification × 40). Arrows, colocalization of signals; asterisks, tubular lumen. Immunohistochemistry of (**c**, **d**) Ngal, (**e**) aquaporin 1 (AQP1), and (**f**) Tamm-Horsfall protein (THP) in the mouse kidney treated with (**d**, **f**) unilateral ureteral obstruction (UUO) and in the (**c**, **e**) contralateral kidney (UUN) at 1 day after operation (original magnification, × 20). Serial sections were analyzed.

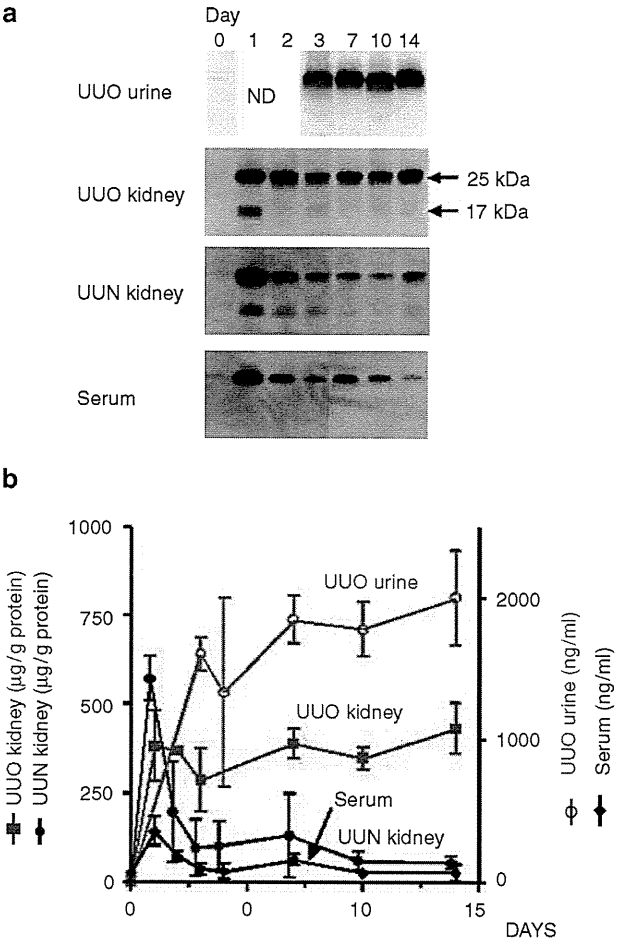

Figure 8 | Ngal protein levels in UUO, UUN, serum, and urine in mice with kidney obstruction. (**a**) Western blot analysis of Ngal protein. ND, not determined. (**b**) The mean Ngal concentrations in UUO, UUN, serum, and urine (collected from dilated pelvis of the UUO side using a needle and syringe). Elevation of Ngal concentrations were statistically significant at day 1 in UUO or UUN kidneys and serum, and at day 3 in urine ($P<0.01$ by unpaired *t*-test, $n=3$) compared to day 0 (no operation).

reabsorbed very efficiently by proximal tubules, leaving only 0.1–0.2% in the urine.[2] By analyzing renal handling of exogenously injected Ngal, the present study emphasized the existence of tubular reabsorption impairment in diabetic nephropathy.[28] In reverse, cellular stress in the proximal tubules may cause deterioration in diabetic nephropathy, as it was reported that transgenic overexpression of catalase in the proximal tubules of mice attenuated development of hypertension and albuminuria associating diabetic nephropathy.[29]

Treatment of STZ-diabetic mice with ARB significantly reduced urinary excretion of both Ngal and albumin. Two major scenarios can be proposed. First, ARB directly improved reabsorption efficiency in the proximal tubules, which may be mediated by increased peritubular capillary blood flow[30] and by amelioration of oxidative stress.[31] Second, ARB reduced intraglomerular hypertension and hyperfiltration,[32] reduced albumin leakage from glomeruli, and the total amount of the ligands for the common scavenger receptor megalin was decreased in the tubular lumen. This may increase the ratio of Ngal and albumin endocytosed at proximal tubules.

Here we used high-dose STZ to induce a model of diabetic nephropathy. Direct toxicity of STZ to proximal tubules may have exaggerated the elevation of urinary Ngal levels in these mice (which is 77-fold of control mice).[33] Hyperfiltration is reported in rodents given STZ.[32] In a previous report, threefold elevation in creatinine clearance was observed in C57BL/6 mice after treatment with STZ, but serum creatinine levels were not significantly decreased, likely due to concomitant osmotic diuresis and dehydration.[34] In the present study, hyperfiltration may have similarly occurred in STZ-diabetic mice. Growth arrest and leanness of STZ-diabetic mice may be partly related to selective reduction of serum Ngal levels (but not serum creatinine and BUN levels) in the present study, as obesity has been shown to be associated with elevated circulating Ngal levels.[35]

We also observed abundant urinary Ngal excretion in 4 patients with nephrotic syndrome. The mechanism may involve direct competition between Ngal and albumin at the surface of megalin molecule for receptor-mediated endocytosis[26,36] and also general malfunctioning of proximal tubules because of

Table 2 | Changes of urinary biomarker levels in case 5 (interstitial nephritis)

Days after admission	9	37	Fold difference[a]	Normal value
uNgal/uCr (μg/gCr)	256.6	25.4	10.1	<10 μg/l[b]
uProt/uCr (g/gCr)	0.381	0.052	7.3	<0.15 g/day
uβ2MG/uCr (mg/gCr)	18.2	2.8	6.5	<0.3 mg/l
uα1MG/uCr (mg/gCr)	46.4	17.2	2.7	<15 mg/l
sNgal (μg/l)	224	90	2.5	<106 μg/l[b]
uNAG/uCr (U/gCr)	21.1	8.7	2.4	<7 U/l
BUN (mg/100 ml)	15	11	1.4	<22 mg/100 ml
sCr (mg/100 ml)	1.2	1.0	1.2	<1.1 mg/100 ml[c]

MG, microglobulin; NAG, *N*-acetyl-β-D-glucosaminidase; Prot, protein; u and sNgal, urinary and serum Ngal; uCr, urinary creatinine.
[a]Fold difference between days 9 and 37.
[b]Value suggested by ELISA kit supplier.
[c]<1.1 for man and <0.8 for woman.

protein overload. Furthermore, a fraction of urinary Ngal may originate from renal synthesis in addition to reabsorption defect, but Ngal gene expression in human samples was not investigated in this study. The time required for urinary Ngal reduction was variable among cases: ranging from 2 weeks (cases 1 and 2) to more than a month (cases 3 and 4).

In a case with interstitial nephritis, urinary Ngal showed the largest fold increase and the quickest response to steroid treatment in comparison to other urinary biomarkers: total protein, α1- and β2-microglobulins and *N*-acetyl-β-D-glucosaminidase. These findings suggest that urinary Ngal might be particularly useful in the evaluation of kidney recovery in patients with low-grade proteinuria.

To summarize, urinary Ngal is a rapid biomarker of kidney injury and recovery showing a large fold-increase or decrease during clinical course of various renal disorders. Proteinuria seems to be one of important factors affecting Ngal'uria.

MATERIALS AND METHODS

Animal experiments

All animal experiments were conducted in accordance with our institutional guidelines for animal research. Male A-ZIP/F-1 heterozygous transgenic mice and control FVB/N littermates were used at 10 months of age, when A-ZIP/F-1 mice exhibit diabetic nephropathy with massive proteinuria.[18–20] Other animal experiments were carried out with male C57BL/6J mice (Japan Clea, Tokyo, Japan) starting at 8 weeks of age, when they weighted 21–23 g. Diabetes was induced by intraperitoneal injection of STZ (180 mg/kg of body weight; Sigma, St. Louis, MO, USA) in citrate buffer (pH 4.6) and control mice received only citrate buffer. Blood pressure was measured by the indirect tail-cuff method with MK-2000ST (Muromachi Kikai, Tokyo, Japan). Urine samples were collected with metabolic cages. Urinary albumin was measured with murine albumin ELISA (Exocell, Philadelphia, PA, USA). Serum and urinary creatinine levels were assayed by the enzymatic method (SRL, Tokyo, Japan). This method gives reliable measurement when compared to high-performance liquid chromatography method, even in low concentration materials, and performs much better than Jaffe's colorimetric method.[37] Blood glucose and HbA1c levels were determined in tail vein blood at *ad libitum*-fed conditions using Glutest Ace (Sanwa Kagaku, Nagoya, Japan) and DCA2000+ Analyzer (Bayer Medical, Tokyo, Japan), respectively. Mice were killed under pentobarbital anesthesia before organ collection. Prodrug of candesartan, candesartan cilexetil (TCV-116; Takeda Chemical Industries, Osaka, Japan), was initially dissolved at 10 mg/ml in a solution containing 16% polyethylene glycol no. 300 (vol/vol; Nacalai, Kyoto, Japan), 16% ethanol (Nacalai), and 0.7 M Na_2CO_3, and further diluted in drinking water to be given at a final dose of 10 mg/kg/day. This treatment method[38] gave less blood pressure lowering effects compared to gavage administration as previously described.[39] For UUO, mice were anesthetized with pentobarbital, the left kidney was exposed by midline incision, and the left ureter was ligated with 4–0 silk at two points.[40] Mice were killed 1–14 days after the operation.

Recombinant Ngal injection and detection

To investigate renal reabsorption of Ngal, 200 μg of 6 × histidine-tagged (at the C terminus) or 60 μg of Alexa Fluor 546 (Molecular Probes, Eugene, OR, USA)-labeled recombinant mouse Ngal (expressed in BL21 strain of *Escherichia coli*)[2] was injected into the peritoneum of mice. Urine samples were collected for 12 h after His-tagged Ngal injection. Urinary excretion of administered His-tagged Ngal was evaluated by Western blot analysis described below with anti-His antibody (MBL, Nagoya, Japan) or with goat polyclonal anti-mouse Ngal antibody (R&D Systems, Minneapolis, MN, USA). Kidneys were harvested 30 min after Alexa Fluor 546-labeled Ngal injection, snap frozen, sliced at 10 μm thickness and examined by a fluorescence microscope (IX81-PAFM; Olympus, Tokyo, Japan). The signal-positive areas were measured using MetaMorph 7.5 software (Molecular Devices, Downingtown, PA, USA).

Patients and measurement of human Ngal

Patients who admitted to Kyoto University Hospital for the diagnosis and treatment of renal disorders were enrolled under informed consent. This study was approved by the ethical committee on human research of Kyoto University Graduate School of Medicine. Ngal concentrations in the human serum and urine were determined by sandwich ELISA (AntibodyShop, Gentofte, Denmark) usually after 1000- and 250-fold dilution, respectively.

Western blot analysis

Urine, serum, and proteins extracted from organs were separated by SDS–polyacrylamide gel electrophoresis, transferred onto polyvinylidene difluoride membranes, incubated with primary antibody and detected with peroxidase-conjugated secondary antibody and

chemiluminescence. Serum was passed through 100-kDa cutoff membrane (Microcon YM-100; Millipore, Bedford, MA, USA) to remove immunoglobulins before analysis.[2] The amount of Ngal protein was measured by densitometry. Known amounts of recombinant mouse Ngal protein were used as standards.[2]

Real-time reverse transcription PCR

Total RNA was extracted from mouse kidneys and livers with TRIzol reagent (Invitrogen, Carlsbad, CA, USA) and cDNA in each sample was synthesized by High Capacity cDNA Reverse Transcription Kit (Applied Biosystems, Foster City, CA, USA). The mRNA levels of Ngal were determined using Premix Ex Taq (Takara Bio, Otsu, Japan) and ABI Prism 7300 Sequence Detector with the following primers and probe: Ngal forward, 5′-ggcagctttacgatgtacagca-3′; Ngal reverse, 5′-tctgatccagtagcgacagcc-3′; Ngal probe, 5′-FAM-catcctggt-cagggaccaggaccag-TAMRA-3′. Expression levels of Ngal were normalized by glyceraldehyde-3-phosphate dehydrogenase (internal control) levels, whose primer–probe set was purchased from Applied Biosystems.[41] Standard curve was made by serial dilution of cDNA from UUO kidneys.

Immunofluorescence of Ngal and albumin

Snap-frozen human biopsy samples were sliced at 3 μm thickness, fixed with acetone, and incubated with a solution containing both fluorescein isothiocyanate-labeled rabbit anti-human albumin antibody (Dako, Glostrup, Denmark) and goat polyclonal anti-human Ngal antibody (R&D Systems), followed by incubation with TexasRed-labeled anti-goat IgG (Jackson Immunoresearch, West Grove, PA, USA). The spillover of each signal was negligible.

Immunohistochemistry of Ngal and nephron markers

Mouse kidneys were fixed in 4% paraformaldehyde at 4 °C for 12 h and embedded in paraffin. Renal sections of 4 μm were deparaffined, hydrated, and incubated with 0.3% hydrogen peroxide. Antigen retrieval was performed by 0.05 mol/l citrate buffer (pH 6.0) for 10 min in a water bath heated at 100 °C (for Ngal, AQP1 and AQP2), or in a microwave oven (for THP). After cooling, the sections were incubated with 10% normal donkey or goat serum, followed by goat anti-mouse Ngal (1:300; R&D Systems), rabbit anti-AQP1 and AQP2 (1:200; Chemicon International, Temecula, CA, USA), or rabbit anti-THP antibodies (1:200; Biomedical Technologies, Stoughton, MA, USA). Primary antibodies were visualized with horseradish peroxidase-conjugated secondary antibodies and 3,3-diaminobenzidine tetrahydrochloride. Nuclei were counterstained with hematoxylin.

Statistical analysis

Results are expressed as mean ± s.e. Student's *t*-test was carried out to compare two groups. Statistical significance was defined as $P<0.05$.

DISCLOSURE

All the authors declared no competing interests.

ACKNOWLEDGMENTS

The authors are grateful to Dr O. Gavrilova and Dr M.L. Reitman (Diabetes Branch, NIDDKD, National Institutes of Health, Bethesda, MD, USA) for kindly providing A-ZIP/F-1 mice. We also acknowledge Ms Y. Ogawa, A. Yamamoto and other lab members for assistance. This work was supported by Astellas Foundation for Research on Metabolic Disorders, Kanae Foundation for the Promotion of Medical Science, Kurozumi Medical Foundation, Takeda Science Foundation, Smoking Research Foundation, Salt Science Research Foundation, and by Grant-in-Aid for Scientific Research of Japan Society for the Promotion of Science.

SUPPLEMENTARY MATERIAL

Figure S1. Clinical course of cases with (**a**) lupus nephritis (case 3, LN) and (**b**) crescentic glomerulonephritis (case 4, CrescGN).
Figure S2. Low-power fields showing expression of Ngal and nephron markers in unilateral ureteral obstruction (UUO) and contralateral kidneys.
Figure S3. High-power fields of cortex showing expression of Ngal and nephron markers in UUO and contralateral kidneys.
Figure S4. High-power fields of medulla showing expression of Ngal and nephron markers in UUO and contralateral kidneys.
Figure S5. Clinical course of a case with drug-induced interstitial nephritis (case 5, IntN).
Supplementary material is linked to the online version of the paper at http://www.nature.com/ki

REFERENCES

1. Mori K, Nakao K. Neutrophil gelatinase-associated lipocalin as the real-time indicator of active kidney damage. *Kidney Int* 2007; **71**: 967–970.
2. Mori K, Lee HT, Rapoport D *et al.* Endocytic delivery of lipocalin–siderophore–iron complex rescues the kidney from ischemia–reperfusion injury. *J Clin Invest* 2005; **115**: 610–621.
3. Barasch J, Mori K. Cell biology: iron thievery. *Nature* 2004; **432**: 811–813.
4. Yang J, Goetz D, Li JY *et al.* An iron delivery pathway mediated by a lipocalin. *Mol Cell* 2002; **10**: 1045–1056.
5. Mori K, Yang J, Barasch J. Ureteric bud controls multiple steps in the conversion of mesenchyme to epithelia. *Semin Cell Dev Biol* 2003; **14**: 209–216.
6. Flo TH, Smith KD, Sato S *et al.* Lipocalin 2 mediates an innate immune response to bacterial infection by sequestrating iron. *Nature* 2004; **432**: 917–921.
7. Schmidt-Ott KM, Mori K, Li JY *et al.* Dual action of neutrophil gelatinase-associated lipocalin. *J Am Soc Nephrol* 2007; **18**: 407–413.
8. Mishra J, Dent C, Tarabishi R *et al.* Neutrophil gelatinase-associated lipocalin (NGAL) as a biomarker for acute renal injury after cardiac surgery. *Lancet* 2005; **365**: 1231–1238.
9. Mishra J, Ma Q, Prada A *et al.* Identification of neutrophil gelatinase-associated lipocalin as a novel early urinary biomarker for ischemic renal injury. *J Am Soc Nephrol* 2003; **14**: 2534–2543.
10. Wagener G, Jan M, Kim M *et al.* Association between increases in urinary neutrophil gelatinase-associated lipocalin and acute renal dysfunction after adult cardiac surgery. *Anesthesiology* 2006; **105**: 485–491.
11. Bennett M, Dent CL, Ma Q *et al.* Urine NGAL predicts severity of acute kidney injury after cardiac surgery: a prospective study. *Clin J Am Soc Nephrol* 2008; **3**: 665–673.
12. Devarajan P. Emerging biomarkers of acute kidney injury. *Contrib Nephrol* 2007; **156**: 203–212.
13. Coca SG, Yalavarthy R, Concato J *et al.* Biomarkers for the diagnosis and risk stratification of acute kidney injury: a systematic review. *Kidney Int* 2008; **73**: 1008–1016.
14. Waikar SS, Bonventre JV. Biomarkers for the diagnosis of acute kidney injury. *Curr Opin Nephrol Hypertens* 2007; **16**: 557–564.
15. Nickolas TL, O'Rourke MJ, Yang J *et al.* Sensitivity and specificity of a single emergency department measurement of urinary neutrophil gelatinase-associated lipocalin for diagnosing acute kidney injury. *Ann Intern Med* 2008; **148**: 810–819.
16. Ding H, He Y, Li K *et al.* Urinary neutrophil gelatinase-associated lipocalin (NGAL) is an early biomarker for renal tubulointerstitial injury in IgA nephropathy. *Clin Immunol* 2007; **123**: 227–234.
17. Mitsnefes MM, Kathman TS, Mishra J *et al.* Serum neutrophil gelatinase-associated lipocalin as a marker of renal function in children with chronic kidney disease. *Pediatr Nephrol* 2007; **22**: 101–108.
18. Suganami T, Mukoyama M, Mori K *et al.* Prevention and reversal of renal injury by leptin in a new mouse model of diabetic nephropathy. *FASEB J* 2005; **19**: 127–129.